Strength development and environmental assessment of alkali-activated construction and demolition waste fines as stabilizer for recycled road materials

Strength development and environmental assessment of alkali-activated construction and demolition waste fines as stabilizer for recycled road materials

L. Tefa[1], M. Bassani[1]*, B. Coppola[2], P. Palmero[2]

[1] Department of Environment, Land and Infrastructures Engineering
[2] Department of Applied Science and Technology
Politecnico di Torino, Torino, Italy

Luca Tefa: luca.tefa@polito.it
Marco Bassani (* = corresponding author): +39 011 090 5635, e-mail: marco.bassani@polito.it
Bartolomeo Coppola: bartolomeo.coppola@polito.it
Paola Palmero: paola.palmero@polito.it

ABSTRACT

This study investigates the effects of curing temperature on alkali-activated fine particles of undivided construction and demolition waste (CDW) aggregates. Previous investigations demonstrated that such activated fines can stabilize the whole mixture thereby improving its mechanical properties. To comprehensively investigate the behaviour of the activated fine, its strength and leaching properties under different curing temperatures were compared to those of the four alkali-activated powders of CDW aggregate constituents (concrete, reclaimed asphalt, bricks and tiles, and natural aggregate).

Flexural and compressive strength tests at 28 days of curing were performed on different pastes prepared with different liquid to solid (l/s) mass ratios (0.4, 0.5, and 0.6), and cured at 5, 20, 40, and 80 °C. All components showed satisfactory strength properties for l/s = 0.4, which was found to be optimal. A significant enhancement of the mechanical properties was observed for specimens treated at 80 °C. However, non-negligible strength values were obtained at other temperatures. In particular, the undivided fractions showed satisfactory results and a low variability in properties when cured at average roadside temperatures - 5 to 40 °C. Following leaching tests, the environmental compatibility of alkali-activated materials was deemed satisfactory with the concentration of pollutants considerably below the threshold of the European Council Decision 2003/33/EC for non-hazardous waste.

KEYWORDS

construction and demolition waste, alkali-activation, stabilization, mechanical properties, leaching

HIGHLIGHTS

- Alkali-activation (AA) of CDW fines (concrete, asphalt, bricks and tiles, natural aggregates).
- Potential of the undivided CDW fraction to undergo alkaline activation.
- Acceptable strength development at roadwork laying temperatures.
- AA-CDW undivided fines are classifiable as non-hazardous wastes.
- AA-CDW undivided fines is a stabilizing agent for recycled aggregate for subbase pavement layers.

1. INTRODUCTION

The production of waste from construction and demolition activities continues to grow worldwide. Around one-third of the waste annually generated in the EU (i.e. 905 million of tonnes in 2016) derives from the construction, renovation, and demolition of building and civil infrastructures [1]. Construction and demolition waste (CDW) is converted into recycled aggregate through separation, cleaning, and crushing operations in treatment plants, and employed as alternative aggregate and filling material in the civil engineering sector. CDW aggregate derives from a variety of materials with different levels of toughness and hardness, depending on the origin of the waste. In particular, undivided CDW aggregate usually contains particles of recycled concrete (RC), reclaimed asphalt pavement (RA), ceramic products such as crushed bricks and tiles (BT), natural aggregates and excavated soils (NA), and occasional limited quantities of impurities (i.e. gypsum, wood, plastic, paper, metals) [2].

Several studies showed encouraging results from the use of CDW aggregate in total or partial substitution of primary resources in many civil applications [3]; [4]; [5]. Due to the large volumes involved, the greatest amount of CDW aggregate is used in the construction of subgrades and embankments of low to medium trafficked roads [6]. To make CDW aggregates suitable for use in the structural layers of road pavements (i.e., subbase and base) of trafficked roads, they must first be stabilized.

Several experimental investigations proposed the stabilization of CDW aggregates with ordinary Portland cement (OPC) [7]; [8]; [9]; [10]. However, concerns relating to the environmental sustainability of OPC [11] have resulted in researchers shifting their attention towards the use of supplementary cementitious materials (e.g., fly ashes, cement kiln dust [12]; [13]; [14]) or alternative binders such as sulfoaluminate cement, alkali-activated materials, and geopolymers [15]; [16]; [17]; [18]; [19].

In particular, geopolymers and alkali-activated materials are attracting great interest thanks to the possibility of achieving hardened products with physical and mechanical properties comparable to cementitious ones, starting from several by-products as precursors [19]; [20]; [21]; [22]; [23]. According to Davidovits [24], geopolymers have a three-dimensional polymer structure deriving from the dissolution of silica and alumina species and subsequent condensation phenomena. On the other hand, alkali-activated materials are produced by adding highly reactive powders to the alkaline activator, resulting in high-strength materials with hydrated and/or precipitated products [20]; [21]; [22]. The precursors in the alkali-activation process are mainly silica and alumina rich materials, but ferrous or non-ferrous slags, calcined clay, natural pozzolans, Ca-rich materials and many other by-products have been exploited as well [19]; [20]; [22]; [23]; [25]; [26]; [27]; [28].

Recently, the authors of this research adopted two innovative approaches, one which implies the alkali-activation of mineral waste with a highly crystalline structure [29]; [30], the second that uses CDW fines [31]; [32]. To date, previous studies have employed CDW aggregate as a reinforcement in alkali-activated materials [33], or have explored the feasibility of cementitious (RC) and ceramic (BT) components of CDW fines undergoing alkali-activation, exploiting their aluminate and silicate content [34]; [35]; [36]; [37]; [38];

[39]. The majority of these investigations proposed a thermal curing treatment to improve the dissolution of these waste powders in the alkaline medium, and therefore their reactivity [40]; [41]; [42]; [43]; [44]; [45].

To be used in road constructions, any recycled material needs to comply with physical, mechanical and environmental requirements. In fact, in the road pavement, base and subbase layers may interact with rainwater and/or groundwater. Then, there is the need to assess the leachate of harmful substances during the pavement service life [46], since potential hazardous pollutants can dissolve into the percolating water, becoming a potential risk for the environment [47]; [48].

In this research, CDW fines have been used in the alkaline activation process, without the addition of any other binder or supplementary reactive precursors (e.g., fly ash, blast furnace slag) to the raw material. The innovative aspects of this research compared to the literature are multiple. The potential for all constituents of CDW aggregate (also including RA and NA which have not been considered in literature) to undergo alkali-activation has been investigated here. Furthermore, fine particles were differentiated into six fractions and investigated separately. Four were obtained from the milling of the four main constituents of CDW (RC, RA, BT, and NA), one was produced by sieving the fine naturally present in CDW aggregate (named UND1) the composition of which is unknown. Therefore, in order to compare this component with a powder of known composition, the last fraction was composed by mixing particles of RC, RA, BT, and NA in equal measure (named UND2). Thermal treatments at several temperatures (5, 20, 40 and 80 °C, for 48 h) were applied to specimens to understand the effects of different thermal conditions on practical field roadwork applications (temperatures in the field can range from about 5 °C to 40 °C), and to understand the behaviour of the materials with respect to optimal curing conditions for alkaline-activated binders (80 °C) [40].

Compared to a previous author's contribution [32], several factors are new in this investigation: (i) the variable liquid to solid (l/s) mass ratio ranging from 0.4 to 0.6, (ii) the evaluation of the strength development under curing temperatures between 5 and 80 °C; (iii) the addition of the UND2 fraction to evaluate the effects of a different blend of the four basic CDW fine constituents, and (iv) the evaluation of the environmental compatibility of alkali-activated products as per the leaching test. The experimental design is aimed at assessing the potential of UND1 to undergo alkali-activation and be effectively used as a precursor in the stabilization of CDW aggregate for the granular base and subbase pavement layers of heavily trafficked roads.

2. MATERIALS AND METHODS

2.1 Materials

Undivided CDW aggregates in the 0-25 mm size fraction were collected from the Cavit S.p.A. plant located in the metropolitan area of Turin (North West of Italy). This recycling plant processes waste generated from the micro demolition and renovation of buildings and civil infrastructures through selection, crushing, cleaning, and sieving operations. According to Bassani and Tefa [49], in the Turin area several recycling plants produce undivided CDW aggregate, which is predominantly made up of RC and NA particles (70-95%wt), and of a significantly lower amount of RA and BT (5-30%wt). Less than 1%wt was made up of impurities (wood, glass, plastic and paper). Variations in proportions derive from the unselected reception of both

demolition and construction wastes. The volume of a particular constituent present depends on the source of the material (construction and demolition of buildings, pavement renovation, pavement cuts and repairs, earthworks). As a result, CDW composition may vary between plants and even within the same plant over time.

From collected CDW aggregates (0-25 mm), the undivided fine sample (named UND1), which is an unknown mixture of the four main constituents, was obtained by sieving operations. More specifically, two different size fractions $d < 0.063$ mm and $0.063 \leq d < 0.125$ mm were selected according to Komnitsas et al. [40], who indicated that particles finer than 0.150 mm are more reactive under alkali-activation. Particles of these two size fractions were combined in equal measure (50% of mass each) to form the initial precursor powder, in accordance with a previous investigation [32].

With the aim of comparing the properties of AA UND1 with those of the four main constituents (RC, RA, BT, and NA), samples of the constituents in powder form were individually subjected to AA. Particles of RC, RA, BT and NA larger than 10 mm were visually separated from each other and then pulverized in a hollow drum. About 3 kg of separated constituent powders were placed into the Los Angeles abrasion machine together with 15 steel balls of 430 g each (at a speed of 33 rpm for 45 minutes). In the end, each powder was sieved at the 0.063 and 0.125 mm openings to obtain the two $d < 0.063$ mm and $0.063 \leq d < 0.125$ mm fractions. Consistent with the treatment of the UND1 sample, these two fractions were then mixed in equal measure (50% of mass each) (Figure 1). Since UND1 is an undefined combination of RC, RA, BT, and NA fines with minor quantities of unidentified impurities, a sixth fraction named UND2 was prepared by combining in equal parts (25% each) RC, RA, BT, and NA fines already mixed in the two size fractions ($d < 0.063$ mm and $0.063 \leq d < 0.125$ mm). The compositional proportion of UND2 powders was selected to have a precursor containing the main constituents (RC, RA, BT, NA).

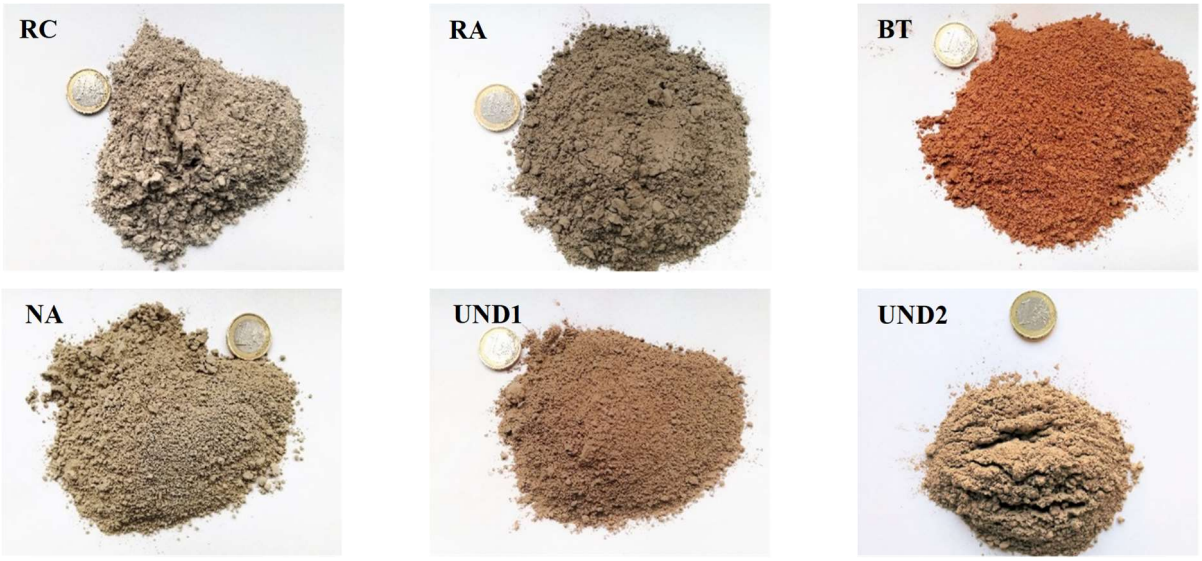

Figure 1 - Fines from CDW powders separated into their main constituents (RC, RA, BT, NA) together with mixtures (UND1, UND2)

The alkaline solution used to activate the above powders was produced in two stages. Firstly, anhydrous flakes of sodium hydroxide (NaOH, purity > 98%, Sigma Aldrich) were diluted in distilled water at 50 wt%. Secondly, sodium silicate (Na_2SiO_3, Ingessil s.r.l., Italy), already in liquid form and characterized by a SiO_2/Na_2O mass ratio of 3.4 (i.e., SiO_2 = 28.1%, Na_2O = 8.4%, H_2O = 63.5%) and a pH of 11.6, was added to the NaOH solution in a 4:1 mass ratio, to produce the final activating solution [29]; [32].

2.2 Characterizations of CDW fines

X-ray diffraction (XRD) analyses were performed on raw powders (d < 0.063 mm) by using a Pan'Analytical X'Pert Pro instrument (Pan'Analytical, Almelo, The Netherlands) with CuKα radiation (0.154056 nm) in the 2θ range 5-70°. As evident from Figure 2, all the raw fines were composed of well-crystallized phases. All fractions were characterized by the presence of quartz, whose main peak (located at 26.65° 2θ) shows a predominant intensity over the XRD reflections of all other phases. Calcite (main peak at 29.405° 2θ) was also present in all the samples, showing the strongest peak intensity in RC and NA samples, and the lowest one in BT, as expected in this waste source [50]. In addition, several aluminosilicate phases (such as albite, illite, phlogopite, lizardite, cordierite, clinochlore, muscovite) were detected in all fractions. Outside of some expected differences in peak intensities, the indexed phases are generally in good agreement with a previous work [32].

The chemical composition of the starting powders (in particular that of the smaller size fraction, which is supposed to be the more reactive under alkaline conditions) was investigated by X-ray fluorescence (XRF, Rigaku ZSX 100E) analysis. According to the results reported in Table 1, all the fractions contain a significant amount of SiO_2 and Al_2O_3, suggesting their potential for alkali-activation. BT is characterized by the largest amount of alumina and silica, in addition to a relevant amount of Fe_2O_3, which explains the reddish appearance of this ceramic waste [51]. Moreover, the role of Fe species in the alkali-activation process has been investigated by several authors, showing that the production of ferrosialates (Fe(Al)–S–H) can also contribute to the achievement of high-mechanical properties [19]; [23]; [52]; [53]. The elemental composition of BT is in line with previous literature: the amounts of SiO_2 (59%) and Al_2O_3 (18%) are in broad agreement with the range 50-66% and 9-21% reported for these two oxides, respectively [44]; [54]. Consistently with Allahverdi and Kani [34] and Puthussery et al. [55], a significant amount of CaO is detected in RC as a consequence of residual cement and calcium-rich aggregate included in this component [56]. A comparable elemental composition can be evinced by the UND1 and UND2 fractions, with significant quantities of silica (45 and 47%, respectively) and alumina present (greater than 14% and 10% for UND1 and UND2 respectively). These values are consistent with previous results [57]; [58]; [59]; [60].

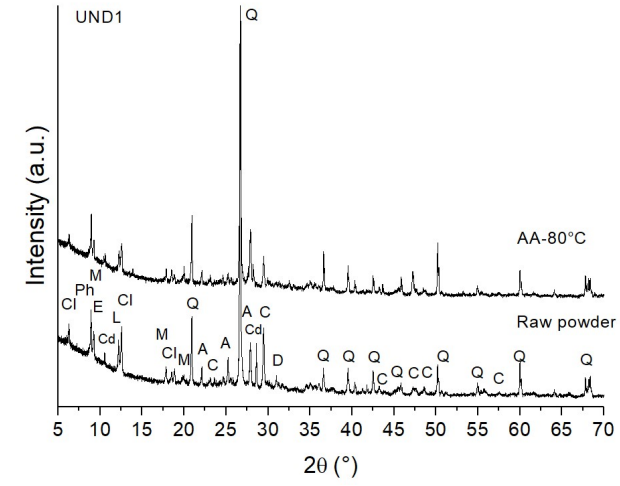

(a)

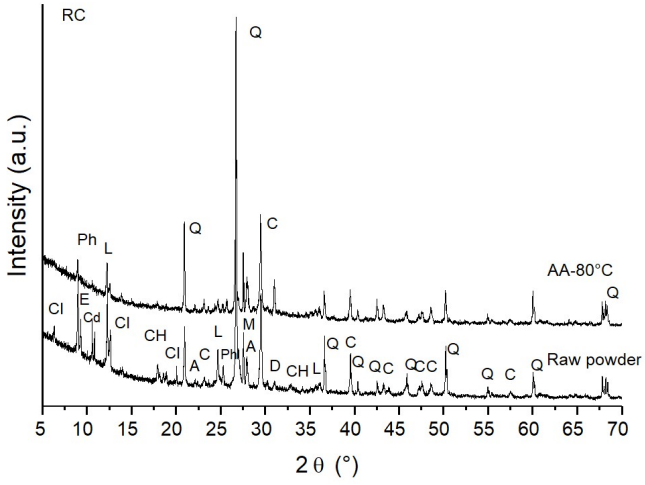

(b)

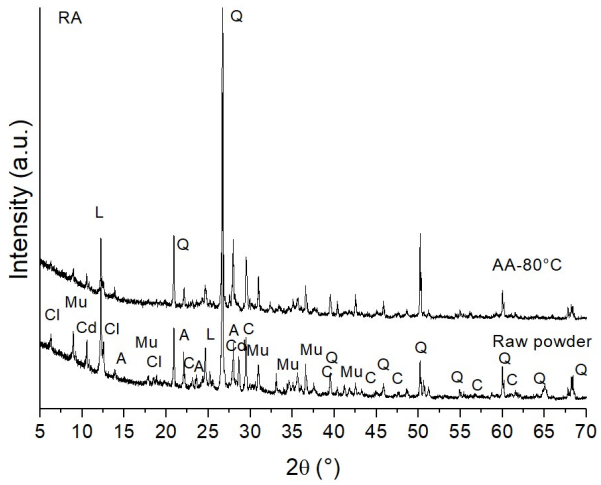

(c)

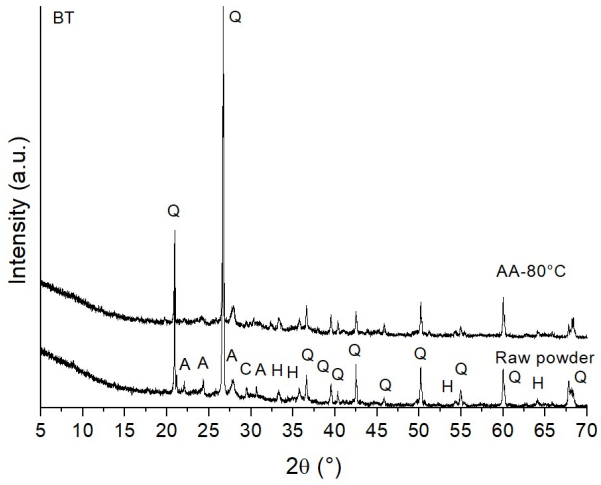

(d)

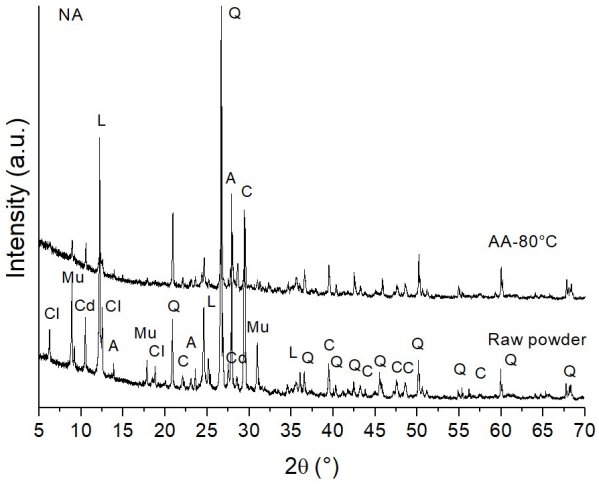

(e)

Figure 2 - XRD patterns of (a) UND1, (b) RC, (c) RA, (d) BT, and (e) NA raw powders and alkali-activated pastes cured at 80°C (AA-80°C). Q = quartz; C = calcite; A = albite; L = lizardite; Cl = clinochlore; Ph = phlogopite; Cd = cordierite; CH = portlandite; E = ettringite; M = microcline; Mu = muscovite; H = hematite.

Table 1 - XRF results of CDW fines

Element	Mass (%)					
	RC	**RA**	**BT**	**NA**	**UND1**	**UND2**
SiO_2	36.69	46.49	58.75	43.19	45.15	47.03
Al_2O_3	6.45	9.61	18.19	6.95	14.42	10.30
CaO	25.70	8.01	4.63	16.57	11.53	13.73
Fe_2O_3	3.46	4.12	7.03	4.41	4.84	4.75
MgO	8.21	15.59	5.03	13.94	7.07	10.69
SO_3	1.14	1.38	0.24	0.00	1.73	0.69
K_2O	0.98	1.19	2.48	0.88	2.06	1.38
TiO_2	0.35	0.42	0.95	0.33	0.64	0.51
LOI (1000 °C)	14.02	13.19	1.2	12.38	11.41	10.20

Several authors investigated the dissolution of minerals in alkaline environments attesting to their potential in the alkali-activation process [26]; [61]; [62]; [63]. Konno et al. [62] studied the dissolution of calcite for different NaOH molar concentrations and temperatures, confirming the release of Ca^{2+} ions and the formation of $Ca(OH)_2$ for NaOH concentrations higher than 2 M. Moreover, Cwirzen et al. [61] demonstrated that the presence of limestone enhances the Si and Al dissolution from metakaolin. Finally, Ahmari et al. [63], determined the Si and Al dissolution from copper mine tailing (i.e. crystalline materials mainly composed of quartz, albite and sanidine) for different NaOH concentrations and temperatures. The dissolution of Si and Al was higher at 90 °C than at 60 °C and increased in line with an increase in NaOH molar concentration (from 5 to 15 M). These results confirm the possibility of partially dissolving crystalline materials in alkaline environments, allowing some hydration/precipitation reactions.

A laser granulometer (Fristch Analysette 22) was employed to determine the particle size distribution (Figure 3) of the raw powders for both size fractions ($d < 0.063$ mm and $0.063 \leq d < 0.125$ mm). All fractions show particle size distributions in close proximity to each other, in particular the coarser fraction for which almost superimposable curves are observed. The d_{50} value is in the 13-20 μm range for the finest fraction, and in the 90-102 μm range for the coarser one.

Table 2 exhibits the particle density (ρ_p) values for the different CDW fines, determined by the pycnometer method according to EN 1097-7 [64]. The procedure was carried out on powders obtained by mixing the two size fractions ($d < 0.063$ mm and $0.063 \leq d < 0.125$ mm) at 50%wt. NA and BT particles show the greatest ρ_p values. On the other hand, traces of residual cement binding with aggregate ensure that the RC constituent is characterized by a lower density [65]. Similarly, the low density of RA particles is imputed to the bitumen which has a density of around 1020 kg/m^3 [66]. UND1 and UND2 fines exhibit intermediate density values. However, their densities are slightly higher (for UND1) and lower (for UND2) compared to the weighted average density (2603 kg/m^3) of the previously mentioned four fractions. The intergranular porosity of dry compacts (υ) was determined by means of the Rigden compaction apparatus, according to EN 1097-4 [67], and calculated by using the following formula:

$$\upsilon = \left(1 - \frac{m \cdot 4 \cdot 10^3}{\pi \cdot \rho \cdot h \cdot \alpha^2}\right) \cdot 100 \qquad \text{Eq. 1}$$

where m is the mass of the compacted fines (g), α is the internal diameter of the cylinder mould (mm), ρ is the particle density of the fines (Mg/m^3), and h is the height of the compacted fines (mm).

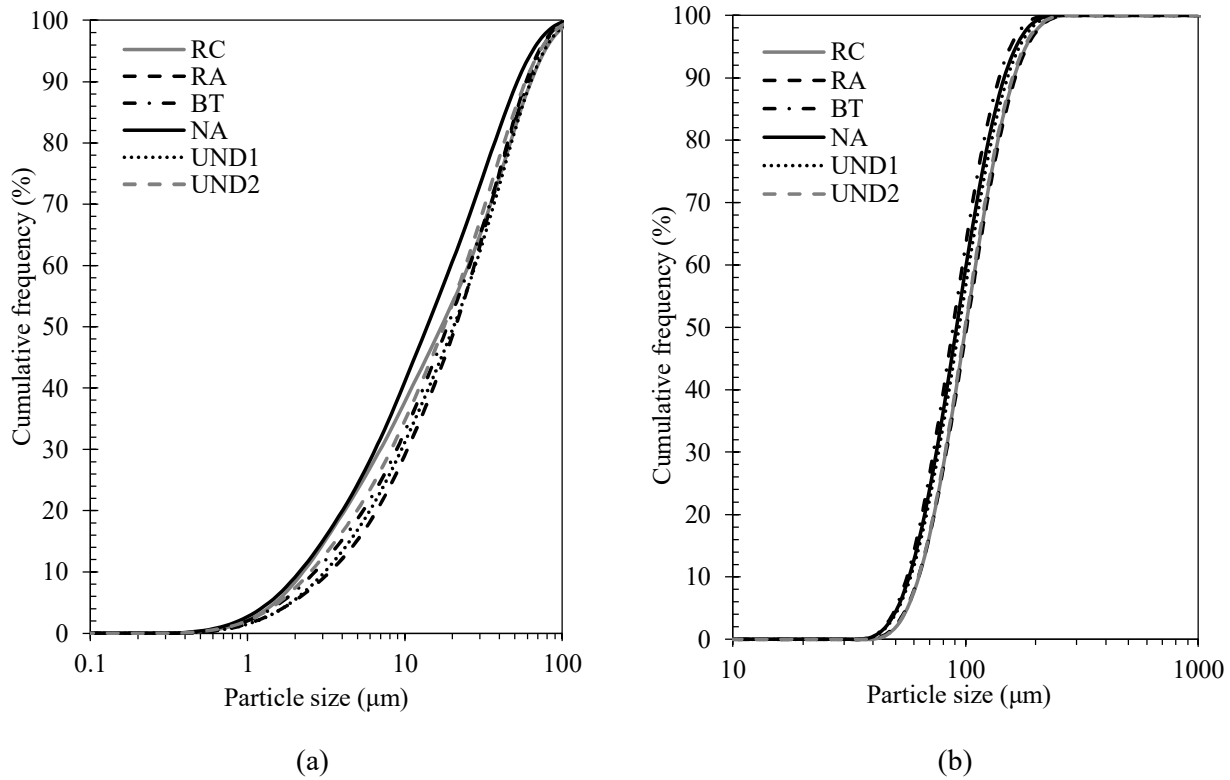

Figure 3 - Particle size distribution of CDW fine fractions: (a) d < 0.063 mm, (b) 0.063 - 0.125 mm

Table 2 - Density of CDW fine particles and intergranular porosity related dry compacts (on powders obtained at 50%wt by mixing the two size fractions)

Constituent	Particle density ρ_p (kg/m^3)	Intergranular dry porosity, υ (%)
RC	2574.0	34.5
RA	2379.5	26.0
BT	2752.0	34.3
NA	2705.0	30.0
UND1	2625.5	33.3
UND2	2565.5	31.2

2.3 Mixture design and sample preparation

Raw powders were mechanically mixed with the alkaline solution. The liquid activator was gradually added and the fresh paste mixed until it achieved a homogeneous appearance. The subsequent experimentation was divided into two phases.

In phase 1, the effect of the solid-to-liquid proportion on the development of mechanical strength values was explored with a view to assessing which proportion resulted in the best mechanical properties. Three different mix-proportions of the liquid activator and the raw powder were considered, with a liquid-to-solid mass ratio (l/s) set at 0.4, 0.5 and 0.6 consistent with literature [38]; [41]. Table 3 summarizes the mass proportion between the solid phase in the two size fractions, and the liquid phase separated into the alkaline solution components (NaOH, Na_2SiO_3, and water). Immediately after mixing, the pastes were cast into prismatic moulds (80×20×20 mm^3) and cured at room temperature (20 °C) for 24 h. Afterwards, the samples were demoulded, and cured for a further 27 days prior to testing.

Once the optimal l/s mass ratio was selected, phase 2 of the experimentation was conducted to investigate the effect of curing temperature on the development of mechanical strength. Specimens were cured

at four different temperatures (5, 20, 40 and 80 °C) for 48 h and then at room temperature prior to testing (total curing time = 28 days). More precisely, specimens were kept at these four temperatures for 48 h, during which samples exposed to 40 °C and 80 °C were kept in plastic bags to prevent water loss.

During a preliminary stage of the investigation, it was observed that AA specimens containing RA, BT, and NA were slower to harden than RC, UND1, and UND2. In this preparatory phase, alkali-activated CDW precursors were cured at 20 °C and RH > 90% and tested after 7 days. Under these curing conditions, RA, BT, and NA materials were not fully hardened, especially in the core of prismatic specimens. Hence, to promote their hardening, AA-RA, -BT, and -NA samples were stored for 5 days at room temperature (20 °C) after the 48-hour thermal treatment (Figure 4). Afterwards, they continued their curing in the humidity-controlled chamber, at 20 °C and RH > 90% for a further 21 days.

Since AA-RC, -UND1 and -UND2 mostly need humid conditions during curing, specimens of these materials were transferred directly into the humidity-controlled chamber (after heat-curing) and kept there for the following 26 days.

Table 3 - Composition of mixtures at the three l/s mass ratios

Component	Subcomponent	Mass percentage (%)		
		l/s = 0.6	l/s = 0.5	l/s = 0.4
Powder	(d<0.063 mm)	31.3	33.3	35.7
	(0.063mm<d<0.125 mm)	31.3	33.3	35.7
	Total	62.5	66.7	71.4
Sodium hydroxide	NaOH	3.8	3.3	2.9
	H_2O	3.8	3.3	2.9
	Total (NaOH + H_2O)*	7.5	6.7	5.7
Sodium silicate	Na_2SiO_3	10.8	9.6	8.2
	H_2O	19.2	17.1	14.6
	Total (Na_2SiO_3 + H_2O)	30.0	26.7	22.9

Notes: * 15 M NaOH

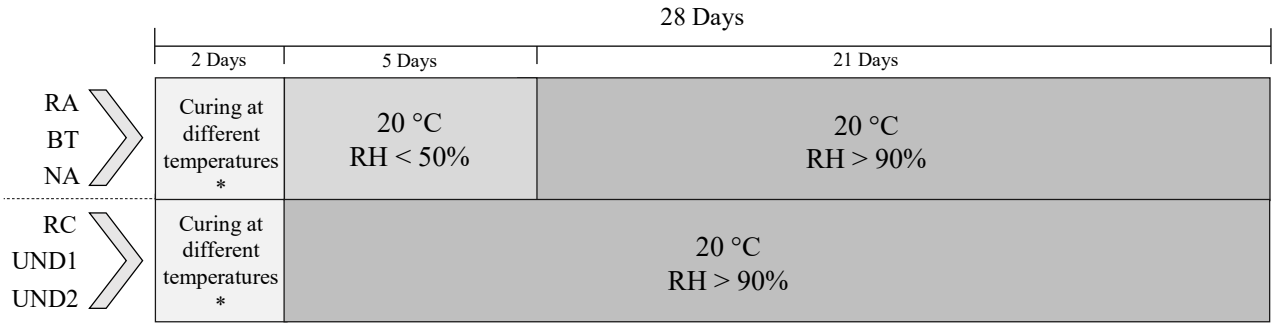

Figure 4 - Curing procedure for the samples prepared in phase 2

2.4 Characterizations of hardened pastes

The specimens were first smoothed and levelled, and then measured and weighed. The effectiveness of alkali-activation was measured in terms of strength development. The flexural strength ($\sigma_{f,max}$) values for five prismatic samples were measured in the three-point bending configuration with a bottom span between

supports equal to 60 mm. Compressive strength ($\sigma_{c,max}$) tests were performed on the two residual pieces obtained after performing the flexural test on ten samples, in accordance with EN 196-1 [68]. An electro-pneumatic testing machine (MTM Zwick/Roell) equipped with a 50 kN loading cell was employed for both flexural and compressive strength tests applying a constant strain rate of 0.25 and 0.5 mm/min respectively. Flexural and compressive strength tests were performed on samples cured for 28 days. In the case of the UND1 and UND2 fractions, the short-term strength development was investigated as well, by performing flexural and compressive strength tests on pastes cured for 7 days. Alkali-activated paste morphologies were examined by means of a FESEM (Zeiss Supra-40, Oberkochen, Germany) on fractured surfaces after sputtering samples with a thin coating of gold.

The leaching tests for RC, RA, BT, NA, and UND1 were carried out according to EN 12457-2 [69]. The leaching procedure adopted in this investigation is representative of the end-of-life scenario since it uses to materials which are not in the monolithic state as it is during the service life. To evaluate the effect of the alkaline solution on the leakage of environmentally harmful substances, the test was performed on both raw and reacted products. Raw fines were subjected to leaching tests in the same size fractions employed for the preparation of specimens (i.e. 50% in mass of fine < 0.063 mm, and 50% in mass between 0.063 and 0.125 mm). On the contrary, hardened specimens (prepared at a l/s equal to 0.4, and cured at 20 °C for 28 days) were first ground with a jaw crusher to reduce the particle size (d < 4 mm). As per EN 12457-2, solid particles were mixed with a leaching agent (distilled water) in a liquid to solid mass ratio of 10 for 24 h. The anion (Cl^-, F^-, SO_4^{2-}) and cation (Cr, Ni, Cu, Zn, As, Se, Cd, Ba, Hg, Pb) concentration in the eluate was determined according to EN ISO 10304-1 [70] and EN ISO 17294-2 [71], respectively. To compare the results with the thresholds of the Council Decision 2003/33/EC [72], concentrations of pollutants in the eluates (in mg/l) were converted into concentrations per each kg of dry solids (mg/kg) as per EN 12457-2.

3. RESULTS AND DISCUSSION

3.1 Effect of the liquid-to-solid (l/s) mass ratio (phase 1)

Figure 5 displays the average specimen density values after 28 days of curing as a function of the l/s mass ratio. The important role played by the l/s mass ratio can be observed: with the sole exception of BT, all other specimens showed the highest density at the lowest l/s mass ratio (i.e. l/s = 0.4). In particular, RC showed a remarkable difference in the range of density values among samples prepared at l/s = 0.4 compared to those prepared at the higher ratios, whose densities were comparable. A similar behaviour was evident with NA, UND1 and UND2 specimens, with the highest density at 0.4, and lower but comparable values at the other two ratios.

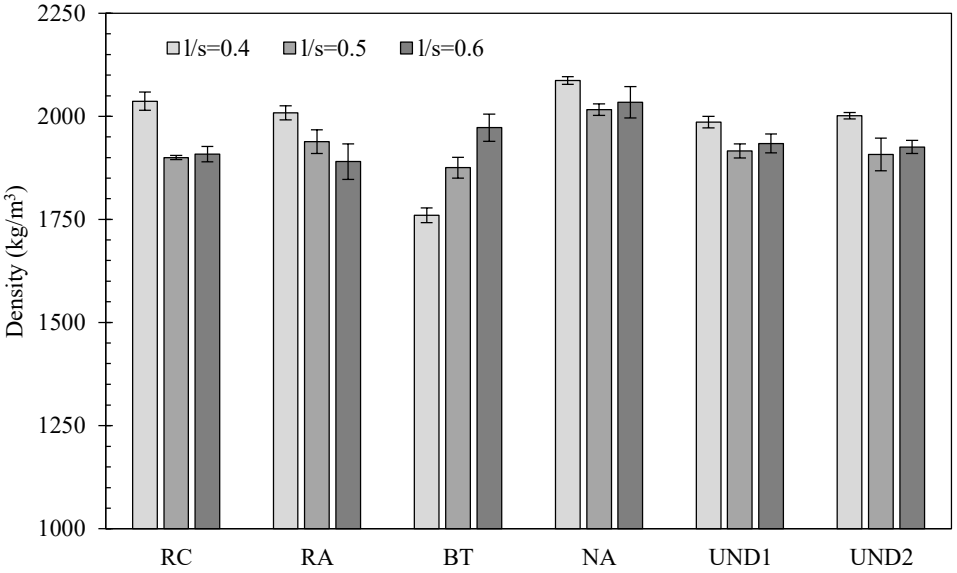

Figure 5 - Average specimen density values after 28 days of curing (at 20 °C only) depending on the l/s ratio (error bars indicate one standard deviation)

Consistent with the particle density (Table 2), AA-NA specimens exhibited the highest density, at all three l/s mass ratios. On the contrary, despite BT powders showing high ρ_p values, even higher than NA ones, when mixed with the alkaline solution and cured for 28 days they displayed a significantly lower density compared to NA specimens. This behaviour could be the result of a weak packing ability due to the irregular morphology of the particles [31]; [73], as confirmed by the high intergranular porosity determined in the dry compact (Table 2). Moreover, the fresh BT paste was difficult to mix and homogenise with l/s = 0.4. As a consequence, a greater number of voids remained in the mixtures, thus resulting in a lower density.

The opposite was true for RA fines: in spite of the lower density of the raw particles compared to the other fractions, the alkali-activated RA pastes were characterized by densities in line with the other materials, suggesting a good packing behaviour of the particles, probably favoured by residual organics. This datum was again strengthened by the low intergranular porosity presented by RA dry compact (Table 2), when compared to the other fractions.

Figure 6a shows the results of the flexural strength test. Average and standard deviation values for each fraction, depending on the l/s ratio, are depicted. RA, BT, NA, and UND1 specimens achieved the highest flexural strength at l/s = 0.4, testifying that, for these components, the excess of liquid phase drastically decreases the development of mechanical strength. For instance, the flexural strength of UND1 samples decreased from 4.2 MPa with l/s = 0.4, to 1.8 MPa with l/s = 0.5, and to 0.3 MPa with l/s = 0.6.

Similarly, the strength of specimens containing BT fines decreased by more than 100% when passing from l/s = 0.4 to 0.5 and 0.6. In the case of RC and UND2, the highest strength was achieved at l/s = 0.5; in spite of this, non-negligible values were obtained at l/s = 0.4, too, while at l/s = 0.6 a drop in the flexural strength occurred.

The compressive test results, depicted in Figure 6b, are consistent with flexural strength trends described beforehand, thus similar considerations can be made. It is worth noting again the important role of

the l/s mass ratio, since lower values are associated with higher strength. In particular, RC, RA, BT, and NA samples show the highest compressive strength at l/s = 0.4, while for UND1 and UND2 specimens, almost comparable values at l/s of 0.4 and 0.5 were recorded. Moreover, at all three l/s mass ratios, RC samples invariably displayed the highest values, and RA the lowest ones, in broad agreement with flexural test results. Considering the results in both Figure 5 and Figure 6, it is worth observing that the higher the density the higher the strength values. Apart from BT, the reduction in strength due to the increase in the l/s ratio can be partially ascribed to the decrease in density of hardened samples. On the grounds of these results, the l/s ratio was fixed at 0.4 and used in the second phase of this experimental study.

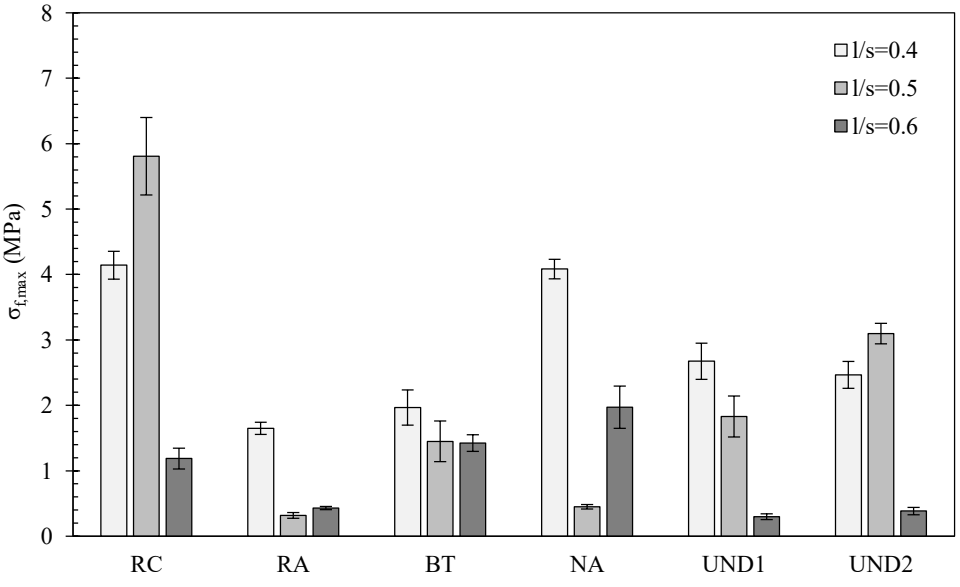

(a)

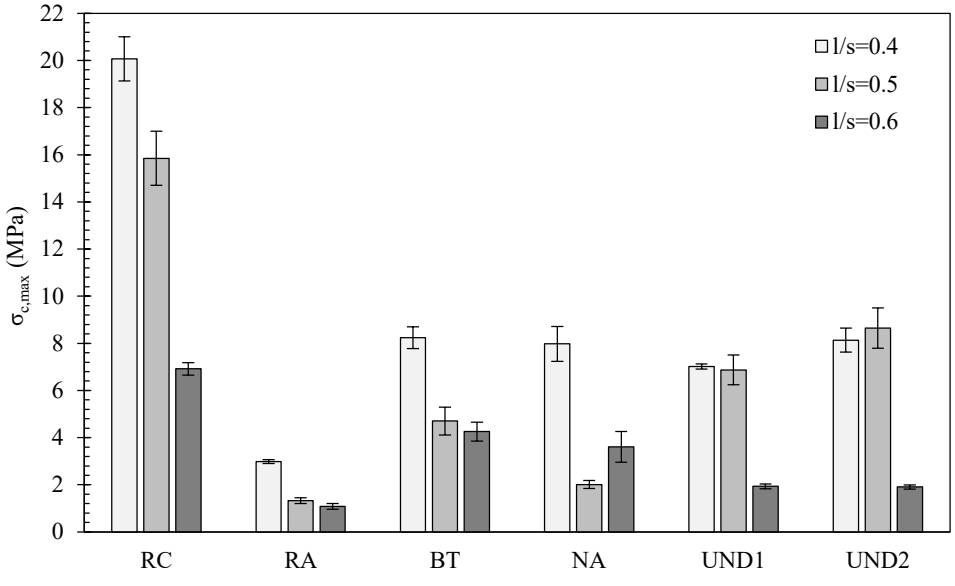

(b)

Figure 6 - Average flexural (a) and compressive (b) strength values for 28-day cured (at 20°C only) specimens made up of CDW constituents and fines, depending on the l/s mass ratio (error bars indicate one standard deviation)

3.2 Effect of curing temperature (phase 2)

The density values of the samples subjected to the different curing conditions are depicted in Figure 7. In line with the previous results, NA samples achieved the highest densities, independently of the curing temperature. On the other hand, BT specimens showed a significantly lower density compared to the other pastes, at all curing temperatures. This behaviour can be explained once again by the poor packing behaviour of BT particles that, when mixed with the alkaline solution, produced a less compact structure. Intermediate values were achieved by the other CDW precursor powder.

Considering the effect of the curing temperature, samples subjected to 80 °C showed the lowest density, probably due to a higher mass loss of water during the first 48h of curing at that temperature. However, in general, it is not possible to ascribe a clear role in sample density to curing conditions, suggesting that the equilibria between water evaporation and absorption (due to the curing atmosphere) probably affected the sample mass values and the drying shrinkages in a complex way.

In Figure 8, the 28-day flexural (Figure 8a) and compressive (Figure 8b) strengths are reported. The key role played by the curing temperature in determining both flexural and compressive strength values can be observed. In fact, all the investigated materials showed the highest strength at the highest curing temperature (80 °C). In particular, this result suggests that a heat-curing treatment is necessary to ensure the dissolution of the mineral phases present in the CDW fines (Figure 2), with these phases being mainly quartz, calcite and aluminosilicates, as already reported in the literature for CDW [40] and other crystalline materials [26]; [63]. In order to have a closer look at the alkali-activation mechanism, the phase composition of the materials hardened at 80 °C was compared to that of the starting powders.

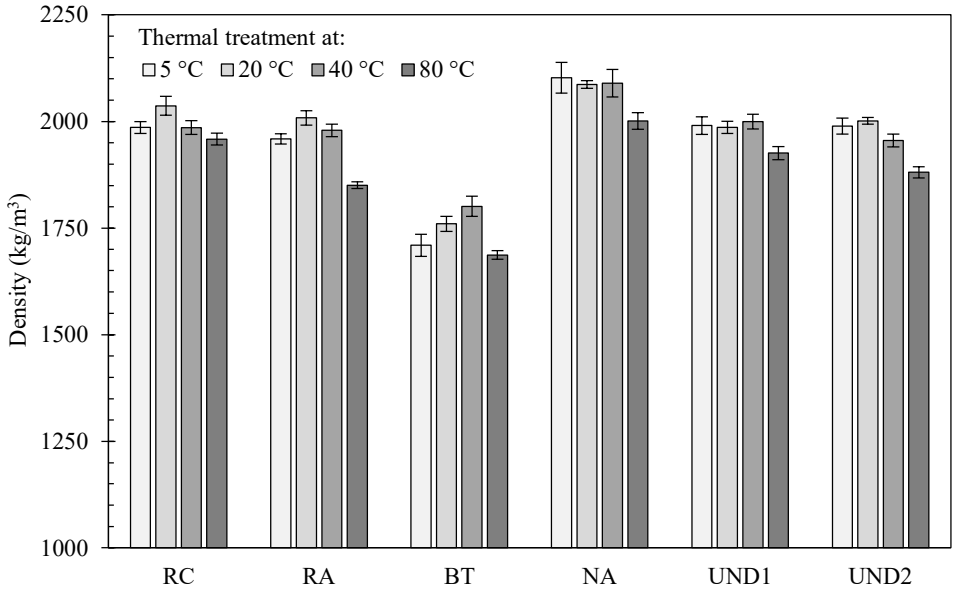

Figure 7 - Average density of 28-day cured specimens (l/s = 0.4) made up of CDW constituents and fines, depending on the curing temperature (error bars indicate one standard deviation)

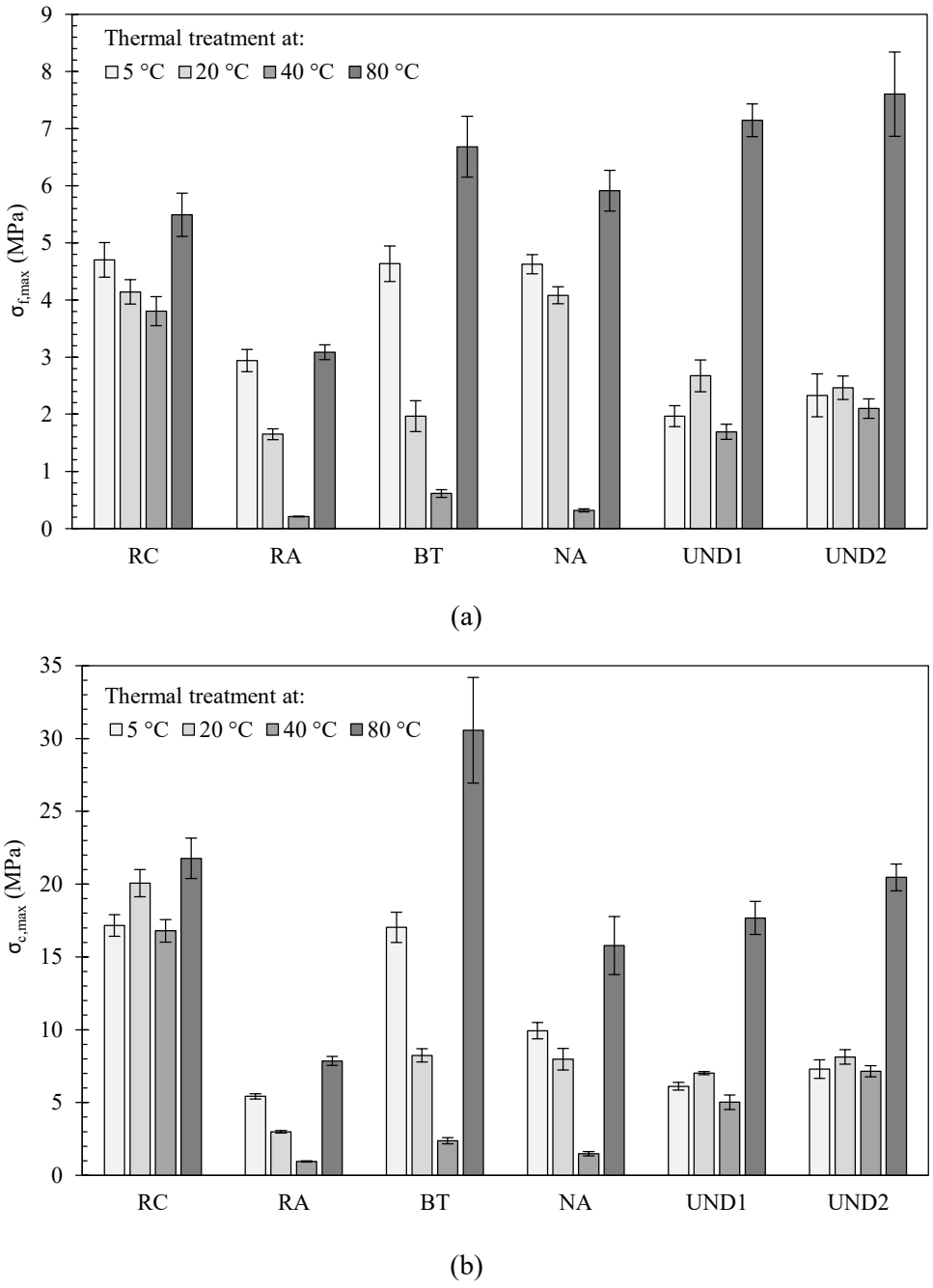

Figure 8 - Average flexural (a) and compressive (b) strengths of 28-day cured specimens (l/s = 0.4) made up of CDW constituents and fines, depending on the curing temperature (error bars indicate one standard deviation)

According to the XRD patterns in Figure 2, it was not possible to clearly recognize the formation of new phases, and the presence of almost identical mineral phases in raw powders and hardened materials can be recognized. However, a general, slight decrease in the crystalline peaks intensity, compared to the respective peaks of the individual raw materials, was observed in the hardened pastes, which was ascribable either to the addition of sodium silicate to the mixtures or to the partial dissolution of the crystalline phases in the alkaline medium [29]; [40]; [74]. Even though no phase quantification is provided here, it was observed that some silicate phases (i.e., muscovite, lizardite, clinochlore, and cordierite) showed the most pronounced decrease in peaks intensity, suggesting their preferential dissolution – among the mineral phases – under alkali-activation conditions [29]. In addition, in the 80 °C cured RC sample, besides the decrease of the previously mentioned

phases, the XRD pattern corresponding to portlandite almost completely disappeared, strengthening the hypothesis of a certain reaction between calcium hydroxide and silica species, leading to the formation of a calcium-silicate-hydrated (C-S-H) gel. It should, however, be clarified that no new XRD signals corresponding to calcium silicate phases were detected in the hardened paste, probably due to their semi-crystalline or nearly amorphous structure [75]. The formation of C-S-H gel in geopolymer systems has been reported by many researchers [76]; [77]; [78] although some of them did not find any C-S-H gel in geopolymeric systems even with added Ca [79]; [80].

None of the investigated compositions showed a progressive trend in strength development following an increase in curing temperature. Thus, a threshold temperature for alkali-activation – and consequently for any increase in mechanical strength – can be supposed, as observed in previous studies [40]; [63]; [81]. Ahmari et al. [63], reported a notable increase in compressive strength values between 75 and 90 °C for copper mine tailings (i.e. crystalline materials composed mainly of quartz, albite and sanidine) activated with an alkaline solution of NaOH (15 M). Similarly, Komnitsas et al. [40], reported on the alkali-activation of different CDW fines (i.e. brick, tiles and concrete) which evidenced the influence of curing temperature and NaOH molar concentration. The optimum curing temperature was found to be 80 °C for tiles and 90 °C for brick and concrete with a remarkable increase in compressive strength moving from 60 to 80-90 °C, confirming the existence of a threshold temperature.

Once again, flexural and compressive trends track each other closely, so similar conclusions from the two tests can be drawn.

RC alkali-activated samples exhibited the lowest dependence on curing temperature. In fact, non-negligible strengths were already achieved in the 5-40 °C curing range, with a further albeit moderate increase at 80 °C. According to the RC chemical composition (Table 1), this fine contains lower amounts of alumina and silica, compared to other fractions, and therefore the effect of heat-curing on the activation of these phases is expected to be less significant. In contrast, the high calcium oxide content of RC can be linked to the presence of residual cement, calcium-rich aggregate [56] and portlandite phase (as detected by XRD analysis). Therefore, the strength development can be a result of the hydration of unreacted cement, and/or the action of calcium on alkali-activated products, implying the formation of calcium silicate hydrate (C-S-H) gel with significant effects on the mechanical properties [82]; [83]; [84].

In the case of BT, NA and RA alkali-activated pastes, a clear decrease in strength when increasing the curing temperature between 5 °C and 40 °C can be observed, with a decrease in the mechanical properties for the mixtures cured at the latter temperature. This behaviour can be explained by considering the role of temperature in the two main possible reactions, i.e. the alkaline activation of fine aluminosilicate particles and the participation of calcium in C-S-H gel formation. As stated, curing at 80 °C favours the former process, leading to the significant increase in strength observed at this temperature [40]. Conversely, curing at a low temperature seems to favour the structural properties of the C-S-H gel [85]; [86]; [87]. In fact, it was postulated that a low hydration rate (such as at 5 °C) might favour the controlled precipitation of reaction products in interstitial space, raising the gel/space ratio, and thus the compressive strength, throughout the curing period

[87]. As a consequence, the curing performed at 40°C corresponds to the least favourable conditions for strength development, thus explaining the decrease in properties observed at this temperature.

UND1 and UND2 samples exhibited a similar behaviour, which was intermediate with respect to those observed for the other fractions. In fact, samples cured in the 5-40 °C range showed comparable strength values, like RC paste, and a significant strength increase at 80 °C, similarly to BT, NA and RA samples.

3.2.1 Comparison with literature

No flexural strength results directly related to the alkali-activation of CDW fines are available in literature to facilitate a comprehensive comparison. However, it is worth noting that some CDW fines (i.e., RC, NA, and UND1) achieved strength values close to the lower range of "traditional" alkali-activated materials prepared from fly ash, blast furnace slag, and metakaolin, which are widely recognized as being highly reactive precursors for the formation of such binders. For instance, blast furnace slag powders activated with an alkaline solution containing Na_2SiO_3, NaOH, and Na_2CO_3, exhibited flexural strength values equal to 5.6, 8.8, and 9.1 MPa after 3, 7, and 28 days of curing at room temperature [88]. Specimens made up of alkali-activated metakaolin (Si/Al ratio of 1.9 and l/s ratio of 0.6) showed $\sigma_{f,max}$ in the range 4.0-6.2 MPa, after 28 days of curing at room temperature [89]. Similarly, Granizo et al. [90] studied two types of metakaolin activated with an alkaline solution at different Na concentrations (from 6 to 20 M). They measured flexural strengths in the ranges 6.3-13.9 MPa and 5.7-10.2 MPa depending on the Na concentration after 2 hours of curing at 80 °C. The results of 3-point bending strength tests carried out by Yamaguchi and Ikeda [91] on alkali activated sewage sludge slag and coal FA ranged between 4.0 and 5.5 MPa, after a curing of 24 hours at 80 °C and of 24 hours at room temperature.

The compressive strength of alkali-activated CDW constituents, mainly RC and BT, has already been investigated in the past. Therefore, an overview of previous results is presented in Table 4, followed by a discussion of the mechanical value results achieved in this work for comparison purposes.

The RC $\sigma_{c,max}$ specimen values (Figure 6b), are slightly lower than those obtained by Vásquez et al. [37] under the same curing conditions (20 °C, 28 days), or under similar heat-curing: in [37], the curing was performed for 24 hours at 70 °C, providing values in the 19.8-26.5 MPa range.

RC specimens achieved higher compressive strengths than those achieved in [38]; [39] under similar curing conditions (80 °C for 24 h), or in [40], in which the curing treatment at 80 °C was extended to 7 days. The combination of (i) the generation of alkali-activated aluminosilicate products and (ii) the formation of C-S-H species ensures that RC samples are blessed with excellent mechanical properties [94]. RC fines were in fact characterized by the highest mass percentage of calcium [95] (Table 1) available for dissolution and corrosion phenomena by the alkaline solution medium. The solubilized calcium together with unreacted silicates in the RC fraction tended to react with water and the silicon species in the alkaline solution, leading to the formation of C-S-H species [74]; [79]; [96].

Table 4 - Compressive strength results of alkali-activated CDW constituents from literature

Author	Material	Activator	l/s ratio	Curing conditions		Tested after (days)	$\sigma_{c,max}$ (MPa)
				Temp.	Time		
Vásquez et al., 2016 [37]	RC	$NaOH + Na_2SiO_3$ (SiO_2/Na_2O=2.70, and SiO_2 content of 32.1 wt%)	0.22	25 °C	28 d	28	11.2÷25.6
			0.22	70 °C	24 h	28	19.8÷26.5
Allahverdi and Kani, 2009 [42]	50% BT + 50% RC	$NaOH + Na_2SiO_3$ (SiO_2/Na_2O=0.86, and SiO_2 content of 34.3 wt%)	0.26	25 °C	28 d	28	12.5÷18.5
	BT		0.30	25 °C	28 d	28	22.5÷40.0
Allahverdi and Kani, 2013 [34]	50% BT + 50% RC	$NaOH + Na_2SiO_3$ (SiO_2/Na_2O=0.86, and SiO_2 content of 34.3 wt%)	0.31	25 °C	28 d	28	15.2÷48.0
	BT		0.33	25 °C	28 d	28	3.2÷16.1
Komnitsas, 2016 [38]	RC	KOH (2÷12 M) + Na_2SiO_3 (SiO_2/Na_2O=3.38, and SiO_2 content of 27.0 wt%)	0.30	80 °C	24 h	7	3.2÷10.0
	BT		0.30	80 °C	24 h	7	8.1÷25.0
Komnitsas et al., 2015 [40]	RC	$NaOH$ (8÷14 M) + Na_2SiO_3 (SiO_2/Na_2O=3.38, and SiO_2 content of 27.0 wt%)	0.48	80 °C	7 d	7	4.2÷5.0
	BT		0.38	80 °C	7 d	7	18.0÷35.0
Robayo-Salazar et al., 2017 [36]	RC	$NaOH + Na_2SiO_3$ (SiO_2/Na_2O=2.70, and SiO_2 content of 32.1 wt%)	0.23	25 °C	28 d	28	10.0÷25.6
	BT		0.23	25 °C	28 d	28	4.0÷54.5
Zaharaki et al., 2016 [39]	RC	$NaOH$ (10 M) + Na_2SiO_3 (SiO_2/Na_2O=3.38, and SiO_2 content of 27.0 wt%)	0.30	80 °C	24 h	7	7.8
	BT		0.30	80 °C	24 h	7	39.4
Pathak and Jha, 2013 [41]	BT	$NaOH$ (6 M) + Na_2SiO_3	0.45	60 °C	24 h	28	11.0
Robayo-Salazar et al., 2016 [45]	BT	$NaOH + Na_2SiO_3$ (SiO_2/Na_2O=2.70, and SiO_2 content of 32.1 wt%)	0.25	25 °C	28 d	28	2.5÷54.5
			0.25	70 °C	28 d	28	6.2÷66.6
Sun et al., 2013 [43]	BT	$NaOH + Na_2SiO_3$ (SiO_2/Na_2O=3.2, and SiO_2 content of 26.5 wt%)	0.40	60 °C	28 d	28	52.2÷63.4
Lampris et al., 2009 [92]	Silt from CDW washing	$NaOH$ (4÷14 M) + Na_2SiO_3 (SiO_2/Na_2O=3.38, and SiO_2 content of 27.0 wt%)	0.26	25 °C	7 d	7	14.0÷18.7
			0.26	60 °C	3 d	7	13.8÷25.9
Jha and Tuladhar, 2013 [93]	Mixed CDW fines	$NaOH$ (5 M) + Na_2SiO_3	0.40	40 °C	15 d	15	7.3

Moreover, the development of C-S-H species was spurred by the sodium silicate in the alkaline solution [97], which acted as a setting accelerator of residual unhydrated cement clinker phases (mainly C_2S which is less reactive than C_3S [98] contained in the RC waste [99]. Indeed, the presence of these unhydrated phases is justified by the fact that the core of bigger clinker particles is not hydrated, and grinding processes create new surfaces and expose them to hydration. However, as stated before, these new hydrated phases were not identified by XRD in the reacted paste. The free water in the solution also favoured the rehydration of unreacted cement particles giving rise to self-cementing phenomena which partially contribute to strength development over time [6]; [100]; [98]. The compressive strengths for the BT samples, cured at 20 °C, were comparable to those reported by Allahverdi and Kani [34] on samples cured for 28 days at room temperature, at a l/s mass ratio of 0.33. However, when this ratio was decreased to 0.30, a further increase was achieved, providing values in the range 22.5-40 MPa [42], and underlining the important role played by the solid content in mechanical strength development. Under the same curing conditions, Robayo-Salazar et al. [45] obtained values up to 54.5 MPa at a l/s mass ratio of 0.23.

BT samples, cured at both 20 °C and 80 °C, achieved higher compressive strength values than those obtained by Pathak and Jha [41] by curing at 60 °C for 24 h. In terms of heat-curing, the highest value that BT specimens achieved here ($\sigma_{c,max}$ = 31 MPa at 80 °C) was close to the values between 25 and 39 MPa obtained at 80 °C for 24 h in [36]; [38]; [39], and at 80 °C after 7 days in [40]. Despite the ceramic fraction being

considered the most alkali reactive CDW constituent due to the high amounts of aluminosilicates [26]; [29]; [30], the results achieved in this work, as well as those in previous literature, clearly state that an effective activation is promoted only at high temperatures (between 60 and 80 °C) [35]; [40]; [43]. Furthermore, if such a heat-curing treatment is prolonged for several days, even higher strength values can be achieved. In fact, by performing a curing treatment at 60 °C [43] or 70 °C [45] for 28 days, compressive strength values in the range 63-67 MPa may be obtained.

UND1 fines at l/s = 0.4 cured at 80°C exhibited compressive strengths slightly lower than those obtained from the alkali-activation of silt generated during CDW washing [90] and cured at 60 °C for 3 days. The gap between literature results and UND1 can be partially attributed to the lower l/s mass ratio (0.26) used in [92]. Better results are presented in [93] for mixed CDW fines, where samples were cured at 40 °C for 15 days.

The results of mechanical tests indicate that fines obtained from the sieving of CDW aggregate (UND1) showed a complete activation at 80 °C. The high content of aluminosilicates and calcite in this fraction (Table 1) suggests the formation of a silica-alumina geopolymer gel, as well as of calcium aluminosilicate hydrated (C-A-S-H) gels that led to a solid network in the structure [101]; [102]. The combined presence of C-S-H hydrates as a result of the reaction between dissolved calcite (from the raw particles), H_2O and Si from the alkaline solution, contributed to mechanical strength development [36]. The FESEM/EDX analysis carried out in [32] on alkali-activated pastes derived from undivided CDW fines showed the presence of a Si-Na based binding phase covering the analysed grains. Besides Si and Na, Al and Ca were detected as well, suggesting their dissolution from the mineral species and diffusion into the matrix, thus contributing to the composition of the binding phase.

While the best (and expected) results were achieved under curing at 80 °C, the strength values achieved under lower curing temperatures were also significant in terms of the stabilization needed in road applications. In fact, flexural strength ranged between 1.5 and 3 MPa, with compressive strength between circa 5 and 7 MPa. Worthy of note is the fact that with respect to other components both the UND1 and UND2 materials showed a lower sensitivity to temperature changes between 5 °C and 40 °C. In fact, in that temperature range a moderate variation in strength was recorded, in contrast to the RA, BT and NA samples, which showed an almost complete loss of properties at 40 °C. As explained, UND1 and UND2 materials take advantage of the specific constituents' behaviour under alkali-activation conditions, which accounts for their higher reliability. When cured at 20 °C, the UND1 paste has already confirmed excellent properties in stabilizing the complete internal structure of CDW aggregate, as previously assessed by the authors in [31].

FESEM micrographs of UND1 alkali-activated samples are reported in Figure 9. A quite dense and well compacted microstructure is visible (Figure 9a) with some undissolved particles still recognizable (Figure 9b). Indeed, after the reaction, the XRD pattern remains mainly crystalline (Figure 2), consistent with FESEM observations. Mechanical properties can be ascribed to the presence of this dense matrix which in turn is a result of hydration and/or precipitation products deriving from the partial dissolution of crystalline phases and

their consequent reaction with the alkaline solution. In addition, good adhesion between unreacted particles and the binding matrix is evident as well.

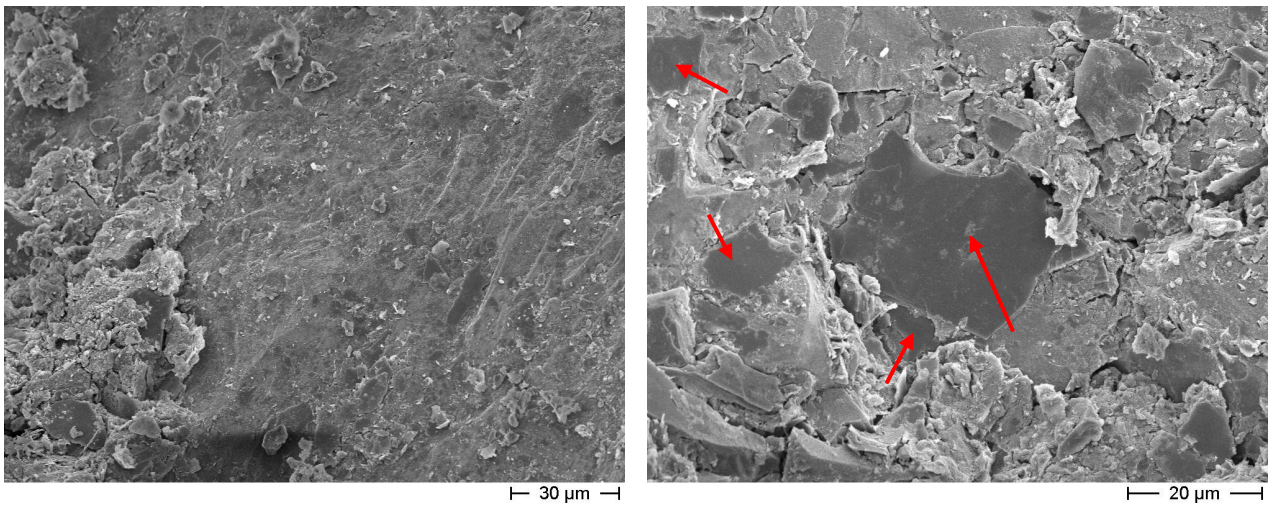

(a) (b)

Figure 9 - FESEM micrographs of 28-day cured UND1 specimens: (a) fracture surfaces and (b) details of undissolved particles (red arrows indicate undissolved particles)

3.2.2 Comparison between undivided samples (UND1 and UND2)

The flexural and compressive strength relationship between UND1 and UND2 constituents is given in Figure 10. For a more comprehensive overview of the mechanical behaviour of these two materials, the flexural and compressive strength values at both short (7 days) and long (28 days) curing times are plotted in these graphs. Strengths developed at 7 days were lower than those at 28 days, except for the samples cured at 40 °C, whose early strength development resulted in values after 7 and 28 days which were very similar to each other. As a further observation on samples tested at 7 days, specimens cured at 5 °C showed a slightly higher strength than those cured at 20 °C. As previously explained, a low-temperature curing probably induced precipitation and gel reinforcement phenomena, which can explain this behaviour.

More in general, all data are well fitted by the equality line, indicating a good correlation between mechanical properties of the two fractions. This suggests that the UND1 fine was probably formed from a homogeneous blend of RA, BT, RC and NA constituents, despite the differences in proportions at the coarser size [49]. However, a closer look at the results shows a slightly better mechanical behaviour for UND2 samples compared to UND1, which can be explained by the slightly higher Si and Ca content in UND2 fines with respect to UND1 (Table 1). Based on this observation, new strategies to further optimize the mix design are envisaged. Starting from a sieved powder from undivided CDW aggregate, the composition could be further optimized by the addition of the other CDW constituents, as well as other more reactive components [103], to achieve higher strength and stabilizing properties.

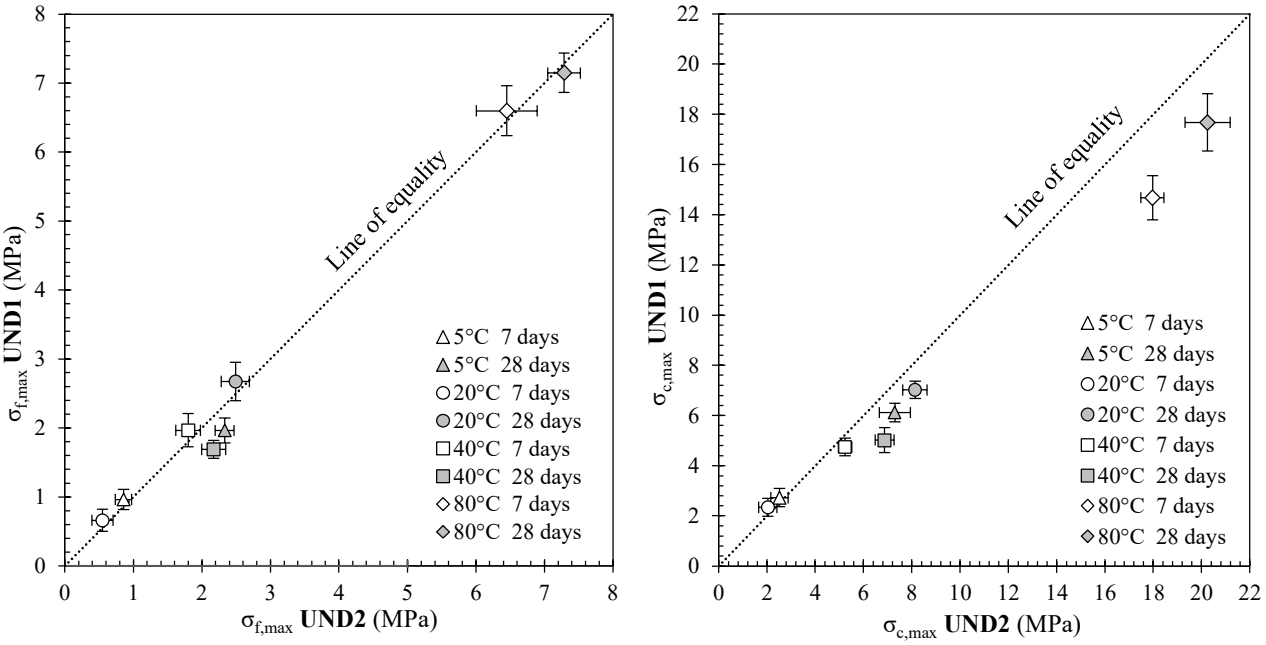

Figure 10 - Strength relationships between UND1 and UND2 fines: flexural (a) and (b) compressive relations (error bars indicate one standard deviation)

3.3 Leaching behaviour

The results of leaching tests on both raw powders and pastes obtained from the alkali-activation of CDW fines are summarized in Table 5, which includes the thresholds of the Council Decision 2003/33/EC [72] for classifying the materials as inert and non-hazardous.

In the case of raw powders, it is evident that CDW fines, before alkali-activation, did not release excessive quantities of harmful substances. The concentration of anions (Cl^-, F^-, SO_4^{2-}) and cations (Cr, Ni, Cu, Zn, As, Se, Cd, Ba, Hg, Pb) are significantly lower than the European threshold [72] for non-hazardous materials. In particular, the concentration of released Cd and Hg was lower than the detection limit of the testing equipment (0.10 μg/l for Cd, and 0.5 μg/l for Hg), and thus can be considered negligible.

Comparing the raw powder data with the EU limits for inert waste, it can be observed that all the fines released a significant amount of chlorides, while still remaining below the acceptance threshold [72]. The same consideration applies to the fluorides, the release of which from RC and BT fines was quite significant but again within EU limits. In contrast, the volume of sulphates released by RC, UND1 and BT breached the acceptance limit (1000 mg/kg) hence these fines should be regarded as inert waste. In particular, the concentration of sulphates from RC fines was five times greater than the aforementioned limit. These results are in partial agreement with XRF data (Table 1), showing a higher amount of SO_3 in UND1, RC, RA raw powders, and a lower quantity in the BT one.

As regards heavy metals, the concentration of chromium released from RC fines (1.08 mg/kg) was two times the limit established in [72] for inert waste (0.5 mg/kg). While BT fines also released a significant amount of chromium (0.42 mg/kg), it was still within the acceptance threshold. Finally, BT showed the largest concentration of barium, with a value of 24.9 mg/kg, slightly exceeding the EU limit (20 mg/kg).

Table 5 - Results of leaching tests (in mg/kg) on both raw and alkali-activated (AA) CDW fines (l/s = 0.4)

Element	EU limits[a]	EU limits[b]	RC		RA		BT		NA		UND1	
			Raw	AA[c]	Raw	AA[c]	Raw	AA[c]	Raw	AA[c]	Raw	AA[c]
Cl^-	800	15000	542	626	430	508	479	533	439	429	496	590
F^-	10	150	6.0	28.1	0.9	4.6	6.8	8.0	2.0	0.0	1.4	7.9
SO_4^{2-}	1000	20000	5325	4718	280	5257	1196	918	788	691	3869	4860
Cr[d]	0.5	10	1.08	1.45	0.01	0.18	0.42	0.23	0.01	0.13	0.04	0.11
Ni	0.4	10	0.00	0.00	0.04	0.67	0.00	0.00	0.04	0.17	0.02	0.50
Cu	2	50	0.08	0.61	0.02	0.41	0.04	0.24	0.02	0.56	0.09	2.00
Zn	4	50	0.01	0.36	0.03	0.82	0.05	0.62	0.03	1.05	0.03	0.50
As	0.5	2	0.01	1.09	0.02	0.58	0.03	1.93	0.01	0.60	0.04	1.56
Se	0.1	0.5	0.01	0.07	0.00	0.03	0.01	0.03	0.00	0.00	0.01	0.03
Cd	0.04	1	n.d.[e]	n.d.[e]	n.d.[e]	n.d.[e]	n.d.[e]	n.d.[e]	n.d.[e]	n.d.[e]	n.d.[e]	n.d.[e]
Ba	20	100	0.98	0.12	7.40	0.32	24.92	0.79	0.89	0.41	0.72	0.70
Hg	0.01	0.2	n.d.[e]	n.d.[e]	n.d.[e]	n.d.[e]	n.d.[e]	n.d.[e]	n.d.[e]	n.d.[e]	n.d.[e]	n.d.[e]
Pb	0.5	10	0.00	0.02	0.00	0.17	0.00	0.59	0.00	0.10	0.00	0.14
pH	-	-	11.0	11.8	8.7	12.2	10.1	11.5	8.3	12.1	8.6	12.0

Notes:
[(a)] threshold of 2003/33/EC [72] for inert waste and L/S=10,
[(b)] threshold of 2003/33/EC [72] for non-hazardous waste and L/S=10,
[(c)] AA = alkali-activation, performed at l/s=0.4 and cured for 28 days,
[(d)] total chromium,
[(e)] n.d. = not detected, since lower than the instrumental detection limit.

The eluates from these fines showed quite a wide range of pH values, from 8.3 to 11.0. RC fines showed the highest pH value (11.0), which can be imputed to the higher amount of CaO in the raw powders, and to the corresponding high level of calcium hydroxide produced in the leachate. This pH value is in the range between 12.5 for fresh concrete and 9.0-10.0 for fully carbonated concrete [104]. In contrast, RA, NA and UND1 showed the lowest pH values. In the case of UND1, this low pH value can be reasonably imputed to the presence of a high proportion of NA particles, as well as to residual clay, soil and silt particles, which are normally characterized by a moderate pH value (in the range 7-8) [105]; [106].

As for the alkali-activated samples, the concentration of both anions and cations are significantly below the European threshold [72] for non-hazardous materials. However, when the same values are compared to the limits for inert waste, none of the compositions meets these requirements.

In fact, the sulphates released from RC, RA and UND1 exceed the EU limit: however, while in the case of RC and UND1 the release from raw powders and hardened materials was comparable, in the case of RA, the amount released from the paste was much larger than from the fines. The chloride concentration was high in all the samples, albeit still within the limits, and showed values in line with those for raw powders. In a number of cases, the heavy metals released from alkali-activated pastes exceeded the EU limits. This was the case with Cr released from RC (1.45 mg/kg), Ni released from RA (0.67 mg/kg), and with Pb released from BT (0.59 mg/kg). Moreover, the As concentration was higher than the EU acceptance limit in all the mixtures investigated. Finally, in spite of the high concentration of barium (Ba) detected in the eluate from the BT fines, a negligible amount was released from the alkali-activated paste.

The pH values determined in the eluates of the alkali-activated materials were in the range 11.5-12.2. As expected, these values were higher than the corresponding pH for the starting powders, but comparable with those for cementitious materials [107].

The results of leaching carried out on raw CDW fines showed that some fractions (specifically, RC, RA, BT and UND1 fines) cannot be considered inert waste, due to some values exceeding the EU limits.

RC fines released the greatest quantities of sulphates and chromium, with these two ions being the most critical substances for acceptance criteria [108]; [109]; [110]. The considerable volume of leached sulphates is mainly attributed to the presence of residual particles of gypsum deriving from gypsum drywall [111]. The chromium concentration is slightly higher than the average values observed by other authors [108]; [109]; [112], while the other elements were released from RC in similar concentrations to previous works [48]; [108]; [109]; [113].

The leaching behaviour of fines made from RA is consistent with previous results [108]; [112], with the concentration of fluorides and sulphates equal to 0.9, and 280 mg/kg respectively.

BT fines are characterized by a significant volume of barium, which is attributed to the addition of barium carbonate ($BaCO_3$) (an anti-efflorescence agent) during the manufacturing of ceramic materials [114]; [115]. In addition, the amount of chromium released by BT is lower when compared with literature [48], while the concentration of Cl^-, F^- and SO_4^{2-} are greater than the values obtained by Saca et al. [116].

As expected, the level(s) of pollutants released by fines from natural aggregate, like NA, were well below the European limits for inert waste. Only in the case of chlorides and sulphates was a certain concentration detected (albeit still within EU limits), due to the fact that NA fines had been in contact with materials of different origin, i.e., cement concrete, ceramics, and asphalt.

Regarding UND1 fines, the only leached substance which failed to satisfy the European requirements for classifying materials as inert was SO_4^{2-}. The excessive volume of sulphates present in CDW aggregate is common in literature due to the presence of gypsum, mortar, and plaster particles in this undivided material [48]; [116]. For instance, 9 out of 10 samples of undivided CDW aggregate analysed by Del Rey et al. [108] exceeded the allowable leached concentration of sulphates (1000 mg/kg) indicated in [72]. Although a more efficient preselection of the material at the treatment plant via the separation of plasters and wallboard is desirable [48]; [113]; [117], there is also the possibility of the biological [118] or chemical [119] removal of sulphates from the leachate of recycled CDW materials.

Concerning the leaching of anions, UND1 released a greater quantity of chlorides and a lower amount of fluorides when compared to literature. Vice versa, the concentration of leached anions is in line with literature data [48]; [108]; [109]; [116].

From leaching test results (Table 5), a generalized increment in the concentration of anions and cations released from alkali-activated CDW fines (pastes) is evident when compared to raw powders.

With the exception of the NA sample, there was an average rise of 15% in the concentration of chlorides in all alkali-activated products. There was also a significant increase in fluorides in alkali-activated RC, RA, and UND1 fines. Specifically, the value of F^- in RC increased from 6.0 to 28.1 mg/kg, exceeding the EU limit for inert waste. A different behaviour was observed in the case of sulphates. The alkali-activation of RC, BT, and NA powders resulted in a reduction in the release of sulphates. The increment of sulphate in the

leachate from AA-UND1 can be attributed to the combination of the slight decrease in AA-RC, -BT and -NA and the significant increase of sulphate released from AA-RA.

Concerning heavy metals, Cr, Ni, Cu, Zn, As, Se, and Pb increased the leached concentrations after alkali-activation. This result can be explained vis-à-vis the following considerations. Firstly, it is worth mentioning that the alkali-activated products – unlike raw powders – underwent a double exposure to the aqueous medium: (i) during the mixing stage and (ii) during the leaching test. During the mixing stage, some substances may be partially released in the liquid phase, and re-precipitated on the particles surface during water evaporation, thus becoming more leachable when further exposed to water. Moreover, the addition of a strong alkaline solution caused a certain level of corrosion in the starting powders [74]; [120], resulting in the structural and compositional destabilization of the material. Therefore, those elements not participating in the alkali-activation process, were more prone to be leached out. More in general, it seems that pH plays a role in the leaching capability of certain substances [121]; [122], regulating their dissolution and adsorption mechanisms. Maia et al. [123] stated that significant amounts of arsenic were released in the eluates at higher pH values. Komonweeraket et al. [124] performed several pH-dependent leaching tests on FA soil mixtures for highway constructions, recognizing that the leaching concentrations of Cr, Zn and Cu were minimal at neutral pH, while the highest concentrations were achieved at both acidic and basic pH conditions.

Among heavy metals, it is worth mentioning the marked reduction in Ba in all the alkali-activated pastes when compared to raw powders. According to Van Jaarsveld et al. [125] and Zhang et al. [126], alkali earth metals (like Ba) tend to be easily dissolved by the alkaline solution and entrapped in the aluminosilicate network of activated products, thus decreasing their leachability. The reduction in Ba can be also ascribed to the higher pH values of reacted products in comparison to raw powders, since some authors reported that the leaching levels for Ba tended to decrease in line with higher pH values [121]; [122].

From the test results in Table 5, it can definitely be concluded that the alkali-activation of CDW fines produced an increase in the quantity of leached substances. Nevertheless, the environmental compatibility of alkali-activated materials may be regarded as satisfactory, since the concentrations of pollutants were below the threshold of the European Council Decision 2003/33/EC [72] for non-hazardous waste, and generally below the threshold for inert ones. It is worth mentioning that in the stabilized material, the paste (i.e., the fine fraction passing at the 0.125 mm sieve opening, and the added alkali solution) represents a fraction which is approximately equal to 20% of the whole mass [31]. Therefore, a significantly lower quantity of anions and cations released by the whole mixture (i.e., the coarse CDW aggregate and the stabilizing paste) in the leachate should be expected, although this needs to be confirmed in future investigations.

The leaching testing method of EN 12457-2 [69] reflects the end-of-life scenario because the material is tested after it has been reduced to a powdery, saturated state. Despite being inadequately representative of in-service conditions, the environmental performance of materials in road applications are still evaluated by referring to the thresholds of the Council Decision 2003/33/EC [72] according to the procedure defined in the EN 12457-2 [2]; [108]; [112]; [127]; [128]. In real conditions, the material is compacted into a dense structure, with a wider particle size distribution and is in an unsaturated state. Thus, real leaching behaviour in the field

should differ with the behaviour observed under laboratory conditions [122], with a significantly lower concentration expected in the latter case. In fact, smaller grains have a greater leaching capability than coarser ones as repeatedly demonstrated in literature [129]; [130]. In view of this, Van der Sloot [131] suggested testing the leaching behaviour of base and subbase road materials in the typical compacted state and in unsaturated conditions with limited infiltration rates.

4. CONCLUSIONS

This experimental investigation aimed at assessing the alkali-activation of the finest particles of CDW aggregates from a mechanical and environmental point of view in order to form stabilized granular base and subbase pavement layers. In contrast to previous studies, the alkali activation potential of all the constituents of CDW fine (< 0.125 mm) aggregate (RC, RA, BT, and NA) was explored. In addition, the finest part (UND1) of undivided CDW aggregate obtained through sieving, together with the fine (UND2) obtained from a mixture consisting of equal parts of the milled powders of the four constituents, were evaluated as precursors in the alkali activation process. Once the optimal liquid-to-solid ratio (l/s = 0.4) for the formulations was selected, the effectiveness of alkali-activation was determined in terms of the mechanical strength values of hardened samples after 28 days of curing at temperatures ranging between 5 and 80 °C. Furthermore, the potential risk of releasing inorganic contaminants into the environment was assessed.

Based on a discussion of the results reported in the manuscript, the following conclusions can be drawn:

- all fractions showed a remarkable (and expected) strength increase when cured at 80 °C for 48 h, confirming that temperature plays a pivotal role in the alkali-activation of the aluminosilicate species present in the investigated CDW fines;
- among all fractions, RC samples showed the lowest sensitivity to high-temperature curing, with significant mechanical values also being achieved in the 5-40 °C range. This behaviour was imputed to further hardening mechanisms, based on the hydration of residual cement and participation of calcium compounds in the formation of C-S-H species;
- the undivided fractions, UND1 and UND2, the composition of which were a blend of all CDW fine constituents, displayed intermediate properties compared to the other components (RC, RA, BT, NA), with an effective exploitation of the hardening mechanisms of each constituent;
- RA, NA and BT showed an almost complete loss of mechanical properties when cured at 40 °C; however, UND1 and UND2 showed satisfactory values and – notably – a low variation in strength in the 5-40 °C temperature range, suggesting a higher reliability of these fractions when exposed to field (i.e., construction site) conditions in road applications;
- finally, the alkali-activation caused a general increment in the level of leached pollutants; however, samples may meet the requirements of the European Council Decision 2003/33/EC (European Parliament, 2003) allowing them to be considered as non-hazardous, thus paving the way towards an

effective exploitation of these wastes as a recycled road material for granular base and subbase pavement applications.

ACKNOWLEDGEMENTS

The authors wish to thank Ms. Maria Jose Rojas Medrano and Mr. Davide Guglielmo for their support with part of this research activity. The UCDW aggregates were provided by Cavit S.p.A. operating in the Turin area (North-west of Italy), while the alkaline solution was provided by INGESSIL S.r.l. (Verona), all of which are gratefully acknowledged for their cooperation and continuous support.

REFERENCES

[1] Eurostat, Waste statistics - Statistics Explained, (2017). http://ec.europa.eu/eurostat/statistics-explained/index.php/Waste_statistics.
[2] J.R. Jiménez, Recycled aggregates (RAs) for roads, in: Handbook of Recycled Concrete and Demolition Waste, Elsevier, 2013: pp. 351–377. https://doi.org/10.1533/9780857096906.3.351.
[3] N. Cristelo, C.S. Vieira, M. de Lurdes Lopes, Geotechnical and Geoenvironmental Assessment of Recycled Construction and Demolition Waste for Road Embankments, Procedia Engineering. 143 (2016) 51–58. https://doi.org/10.1016/j.proeng.2016.06.007.
[4] J. de Brito, A.S. Pereira, J.R. Correia, Mechanical behaviour of non-structural concrete made with recycled ceramic aggregates, Cement and Concrete Composites. 27 (2005) 429–433. https://doi.org/10.1016/j.cemconcomp.2004.07.005.
[5] Md.A. Rahman, M. Imteaz, A. Arulrajah, M.M. Disfani, Suitability of recycled construction and demolition aggregates as alternative pipe backfilling materials, Journal of Cleaner Production. 66 (2014) 75–84. https://doi.org/10.1016/j.jclepro.2013.11.005.
[6] A. Ossa, J.L. García, E. Botero, Use of recycled construction and demolition waste (CDW) aggregates: A sustainable alternative for the pavement construction industry, Journal of Cleaner Production. 135 (2016) 379–386. https://doi.org/10.1016/j.jclepro.2016.06.088.
[7] I. Del Rey, J. Ayuso, A. Barbudo, A.P. Galvín, F. Agrela, J. de Brito, Feasibility study of cement-treated 0–8 mm recycled aggregates from construction and demolition waste as road base layer, Road Materials and Pavement Design. 17 (2016) 678–692. https://doi.org/10.1080/14680629.2015.1108221.
[8] F. Agrela, A. Barbudo, A. Ramírez, J. Ayuso, M.D. Carvajal, J.R. Jiménez, Construction of road sections using mixed recycled aggregates treated with cement in Malaga, Spain, Resources, Conservation and Recycling. 58 (2012) 98–106. https://doi.org/10.1016/j.resconrec.2011.11.003.
[9] P. Pérez, F. Agrela, R. Herrador, J. Ordoñez, Application of cement-treated recycled materials in the construction of a section of road in Malaga, Spain, Construction and Building Materials. 44 (2013) 593–599. https://doi.org/10.1016/j.conbuildmat.2013.02.034.
[10] A. Mohammadinia, A. Arulrajah, J. Sanjayan, M.M. Disfani, M.W. Bo, S. Darmawan, Laboratory Evaluation of the Use of Cement-Treated Construction and Demolition Materials in Pavement Base and Subbase Applications, Journal of Materials in Civil Engineering. 27 (2014) 04014186. https://doi.org/10.1061/(ASCE)MT.1943-5533.0001148.
[11] M. Meyer, M. Hunter, A. Eisenman, Sustainable Streets and Highways: An Analysis of Green Roads Rating Systems, (2012). https://trid.trb.org/view.aspx?id=1246694 (accessed November 28, 2017).
[12] A. Arulrajah, A. Mohammadinia, A. D'Amico, S. Horpibulsuk, Cement kiln dust and fly ash blends as an alternative binder for the stabilization of demolition aggregates, Construction and Building Materials. 145 (2017) 218–225. https://doi.org/10.1016/j.conbuildmat.2017.04.007.
[13] R. Taha, Evaluation of Cement Kiln Dust-Stabilized Reclaimed Asphalt Pavement Aggregate Systems in Road Bases, Transportation Research Record: Journal of the Transportation Research Board. 1819 (2003) 11–17. https://doi.org/10.3141/1819b-02.
[14] M. Bassani, P.P. Riviera, L. Tefa, Short-Term and Long-Term Effects of Cement Kiln Dust Stabilization of Construction and Demolition Waste, Journal of Materials in Civil Engineering. 29 (2016) 04016286. https://doi.org/10.1061/(ASCE)MT.1943-5533.0001797.

[15] K.A. Komnitsas, Potential of geopolymer technology towards green buildings and sustainable cities, Procedia Engineering. 21 (2011) 1023–1032. https://doi.org/10.1016/j.proeng.2011.11.2108.
[16] J.S.J. van Deventer, J.L. Provis, P. Duxson, D.G. Brice, Chemical Research and Climate Change as Drivers in the Commercial Adoption of Alkali Activated Materials, Waste and Biomass Valorization. 1 (2010) 145–155. https://doi.org/10.1007/s12649-010-9015-9.
[17] B.C. McLellan, R.P. Williams, J. Lay, A. van Riessen, G.D. Corder, Costs and carbon emissions for geopolymer pastes in comparison to ordinary portland cement, Journal of Cleaner Production. 19 (2011) 1080–1090. https://doi.org/10.1016/j.jclepro.2011.02.010.
[18] L. Coppola, D. Coffetti, E. Crotti, T. Pastore, CSA-based Portland-free binders to manufacture sustainable concretes for jointless slabs on ground, Construction and Building Materials. 187 (2018) 691–698. https://doi.org/10.1016/j.conbuildmat.2018.07.221.
[19] Y. Pontikes, L. Machiels, S. Onisei, L. Pandelaers, D. Geysen, P.T. Jones, B. Blanpain, Slags with a high Al and Fe content as precursors for inorganic polymers, Applied Clay Science. 73 (2013) 93–102. https://doi.org/10.1016/j.clay.2012.09.020.
[20] F. Pacheco-Torgal, J. Castro-Gomes, S. Jalali, Alkali-activated binders: A review. Part 2. About materials and binders manufacture, Construction and Building Materials. 22 (2008) 1315–1322. https://doi.org/10.1016/j.conbuildmat.2007.03.019.
[21] J.L. Provis, A. Palomo, C. Shi, Advances in understanding alkali-activated materials, Cement and Concrete Research. 78 (2015) 110–125. https://doi.org/10.1016/j.cemconres.2015.04.013.
[22] J.L. Provis, Alkali-activated materials, Cement and Concrete Research. 114 (2018) 40–48. https://doi.org/10.1016/j.cemconres.2017.02.009.
[23] K. Komnitsas, D. Zaharaki, V. Perdikatsis, Geopolymerisation of low calcium ferronickel slags, Journal of Materials Science. 42 (2007) 3073–3082. https://doi.org/10.1007/s10853-006-0529-2.
[24] J. Davidovits, Geopolymers: Ceramic-Like Inorganic Polymers, J. Ceram. Sci. Technol. 08 (2017) 335–350. https://doi.org/10.4416/JCST2017-00038.
[25] L. Coppola, D. Coffetti, E. Crotti, S. Candamano, F. Crea, G. Gazzaniga, T. Pastore, The combined use of admixtures for shrinkage reduction in one-part alkali activated slag-based mortars and pastes, Construction and Building Materials. 248 (2020) 118682. https://doi.org/10.1016/j.conbuildmat.2020.118682.
[26] B. Coppola, J.-M. Tulliani, P. Antonaci, P. Palmero, Role of Natural Stone Wastes and Minerals in the Alkali Activation Process: A Review, Materials. 13 (2020) 2284. https://doi.org/10.3390/ma13102284.
[27] M. Palacios, M.M. Alonso, C. Varga, F. Puertas, Influence of the alkaline solution and temperature on the rheology and reactivity of alkali-activated fly ash pastes, Cement and Concrete Composites. 95 (2019) 277–284. https://doi.org/10.1016/j.cemconcomp.2018.08.010.
[28] X. Gao, Q.L. Yu, H.J.H. Brouwers, Properties of alkali activated slag–fly ash blends with limestone addition, Cement and Concrete Composites. 59 (2015) 119–128. https://doi.org/10.1016/j.cemconcomp.2015.01.007.
[29] P. Palmero, A. Formia, J.-M. Tulliani, P. Antonaci, Valorisation of alumino-silicate stone muds: From wastes to source materials for innovative alkali-activated materials, Cement and Concrete Composites. 83 (2017) 251–262. https://doi.org/10.1016/j.cemconcomp.2017.07.011.
[30] B. Coppola, C. Tardivat, S. Richaud, J.-M. Tulliani, L. Montanaro, P. Palmero, Alkali-activated refractory wastes exposed to high temperatures: development and characterization, Journal of the European Ceramic Society. 40 (2020) 3314–3326. https://doi.org/10.1016/j.jeurceramsoc.2020.02.052.
[31] M. Bassani, L. Tefa, A. Russo, P. Palmero, Alkali-activation of recycled construction and demolition waste aggregate with no added binder, Construction and Building Materials. 205 (2019) 398–413. https://doi.org/10.1016/j.conbuildmat.2019.02.031.
[32] M. Bassani, L. Tefa, B. Coppola, P. Palmero, Alkali-activation of aggregate fines from construction and demolition waste: Valorisation in view of road pavement subbase applications, Journal of Cleaner Production. 234 (2019) 71–84. https://doi.org/10.1016/j.jclepro.2019.06.207.
[33] M. Panizza, M. Natali, E. Garbin, S. Tamburini, M. Secco, Assessment of geopolymers with Construction and Demolition Waste (CDW) aggregates as a building material, Construction and Building Materials. 181 (2018) 119–133. https://doi.org/10.1016/j.conbuildmat.2018.06.018.
[34] A. Allahverdi, E.N. Kani, Use of construction and demolition waste (CDW) for alkali-activated or geopolymer cements, in: Handbook of Recycled Concrete and Demolition Waste, Elsevier, 2013: pp. 439–475.

[35] L. Reig, M.M. Tashima, L. Soriano, M.V. Borrachero, J. Monzó, J. Payá, Alkaline Activation of Ceramic Waste Materials, Waste and Biomass Valorization. 4 (2013) 729–736. https://doi.org/10.1007/s12649-013-9197-z.
[36] R.A. Robayo-Salazar, J.F. Rivera, R. Mejía de Gutiérrez, Alkali-activated building materials made with recycled construction and demolition wastes, Construction and Building Materials. 149 (2017) 130–138. https://doi.org/10.1016/j.conbuildmat.2017.05.122.
[37] A. Vásquez, V. Cárdenas, R.A. Robayo, R.M. de Gutiérrez, Geopolymer based on concrete demolition waste, Advanced Powder Technology. 27 (2016) 1173–1179. https://doi.org/10.1016/j.apt.2016.03.029.
[38] K. Komnitsas, Co-valorization of marine sediments and construction and demolition wastes through alkali activation, Journal of Environmental Chemical Engineering. (2016). https://doi.org/10.1016/j.jece.2016.11.003.
[39] D. Zaharaki, M. Galetakis, K. Komnitsas, Valorization of construction and demolition (C&D) and industrial wastes through alkali activation, Construction and Building Materials. 121 (2016) 686–693. https://doi.org/10.1016/j.conbuildmat.2016.06.051.
[40] K. Komnitsas, D. Zaharaki, A. Vlachou, G. Bartzas, M. Galetakis, Effect of synthesis parameters on the quality of construction and demolition wastes (CDW) geopolymers, Advanced Powder Technology. 26 (2015) 368–376. https://doi.org/10.1016/j.apt.2014.11.012.
[41] A. Pathak, V.K. Jha, Synthesis of Geopolymer from Inorganic Construction Waste, Journal of Nepal Chemical Society. 30 (2013) 45–51.
[42] A. Allahverdi, E.N. Kani, Construction wastes as raw materials for geopolymer binders, Int J Civil Eng. 7 (2009) 154–160.
[43] Z. Sun, H. Cui, H. An, D. Tao, Y. Xu, J. Zhai, Q. Li, Synthesis and thermal behavior of geopolymer-type material from waste ceramic, Construction and Building Materials. 49 (2013) 281–287. https://doi.org/10.1016/j.conbuildmat.2013.08.063.
[44] L. Reig, M.M. Tashima, M.V. Borrachero, J. Monzó, C.R. Cheeseman, J. Payá, Properties and microstructure of alkali-activated red clay brick waste, Construction and Building Materials. 43 (2013) 98–106. https://doi.org/10.1016/j.conbuildmat.2013.01.031.
[45] R.A. Robayo-Salazar, A. Mulford, J. Munera, R. Mejía de Gutiérrez, Alternative cements based on alkali-activated red clay brick waste, Construction and Building Materials. 128 (2016) 163–169. https://doi.org/10.1016/j.conbuildmat.2016.10.023.
[46] M. Wahlström, J. Laine-Ylijoki, A. Määttänen, T. Luotojärvi, L. Kivekäs, Environmental quality assurance system for use of crushed mineral demolition wastes in road constructions, Waste Management. 20 (2000) 225–232.
[47] R. Chowdhury, D. Apul, T. Fry, A life cycle based environmental impacts assessment of construction materials used in road construction, Resources, Conservation and Recycling. 54 (2010) 250–255. https://doi.org/10.1016/j.resconrec.2009.08.007.
[48] A. Barbudo, A.P. Galvín, F. Agrela, J. Ayuso, J.R. Jiménez, Correlation analysis between sulphate content and leaching of sulphates in recycled aggregates from construction and demolition wastes, Waste Management. 32 (2012) 1229–1235. https://doi.org/10.1016/j.wasman.2012.02.005.
[49] M. Bassani, L. Tefa, Compaction and freeze-thaw degradation assessment of recycled aggregates from unseparated construction and demolition waste, Construction and Building Materials. 160 (2018) 180–195. https://doi.org/10.1016/j.conbuildmat.2017.11.052.
[50] D. Kioupis, A. Skaropoulou, S. Tsivilis, G. Kakali, Construction and Demolition Wastes as Resources for the Development of Green Building Materials, in: Proceedings of HISER International Conference Advances in Recycling and Management of Construction and Demolition Waste, 21-23 June 2017, Delft, The Netherlands, 2017.
[51] F. Pacheco-Torgal, S. Jalali, Reusing ceramic wastes in concrete, Construction and Building Materials. 24 (2010) 832–838. https://doi.org/10.1016/j.conbuildmat.2009.10.023.
[52] T. Hertel, Y. Pontikes, Geopolymers, inorganic polymers, alkali-activated materials and hybrid binders from bauxite residue (red mud) – Putting things in perspective, Journal of Cleaner Production. 258 (2020) 120610. https://doi.org/10.1016/j.jclepro.2020.120610.
[53] Y. Hu, S. Liang, J. Yang, Y. Chen, N. Ye, Y. Ke, S. Tao, K. Xiao, J. Hu, H. Hou, W. Fan, S. Zhu, Y. Zhang, B. Xiao, Role of Fe species in geopolymer synthesized from alkali-thermal pretreated Fe-rich Bayer red mud, Construction and Building Materials. 200 (2019) 398–407. https://doi.org/10.1016/j.conbuildmat.2018.12.122.

[54] J. Gonçalves Rapazote, C. Laginhas, A. Teixeira-Pinto, Development of Building Materials through Alkaline Activation of Construction and Demolition Waste (CDW) - Resistance to Acid Attack, Advances in Science and Technology. 69 (2010) 156–163. https://doi.org/10.4028/www.scientific.net/AST.69.156.
[55] J.V. Puthussery, R. Kumar, A. Garg, Evaluation of recycled concrete aggregates for their suitability in construction activities: An experimental study, Waste Management. 60 (2017) 270–276. https://doi.org/10.1016/j.wasman.2016.06.008.
[56] M.C. Limbachiya, E. Marrocchino, A. Koulouris, Chemical–mineralogical characterisation of coarse recycled concrete aggregate, Waste Management. 27 (2007) 201–208. https://doi.org/10.1016/j.wasman.2006.01.005.
[57] G. Bianchini, E. Marrocchino, R. Tassinari, C. Vaccaro, Recycling of construction and demolition waste materials: a chemical–mineralogical appraisal, Waste Management. 25 (2005) 149–159. https://doi.org/10.1016/j.wasman.2004.09.005.
[58] S.C. Angulo, C. Ulsen, V.M. John, H. Kahn, M.A. Cincotto, Chemical–mineralogical characterization of C&D waste recycled aggregates from São Paulo, Brazil, Waste Management. 29 (2009) 721–730. https://doi.org/10.1016/j.wasman.2008.07.009.
[59] P. Saiz Martínez, M. González Cortina, F. Fernández Martínez, A. Rodríguez Sánchez, Comparative study of three types of fine recycled aggregates from construction and demolition waste (CDW), and their use in masonry mortar fabrication, Journal of Cleaner Production. 118 (2016) 162–169. https://doi.org/10.1016/j.jclepro.2016.01.059.
[60] E. Moreno-Pérez, J. Hernández-Ávila, Y. Rangel-Martínez, E. Cerecedo-Sáenz, A. Arenas-Flores, Ma. Reyes-Valderrama, E. Salinas-Rodríguez, Chemical and Mineralogical Characterization of Recycled Aggregates from Construction and Demolition Waste from Mexico City, Minerals. 8 (2018) 237. https://doi.org/10.3390/min8060237.
[61] A. Cwirzen, J.L. Provis, V. Penttala, K. Habermehl-Cwirzen, The effect of limestone on sodium hydroxide-activated metakaolin-based geopolymers, Construction and Building Materials. 66 (2014) 53–62. https://doi.org/10.1016/j.conbuildmat.2014.05.022.
[62] H. Konno, Y. Nanri, M. Kitamura, Crystallization of aragonite in the causticizing reaction, Powder Technology. 123 (2002) 33–39. https://doi.org/10.1016/S0032-5910(01)00424-7.
[63] S. Ahmari, L. Zhang, J. Zhang, Effects of activator type/concentration and curing temperature on alkali-activated binder based on copper mine tailings, J Mater Sci. 47 (2012) 5933–5945. https://doi.org/10.1007/s10853-012-6497-9.
[64] European Committee for Standardization, Tests for mechanical and physical properties of aggregates - Part 7: Determination of the particle density of filler - Pyknometer method, 2008.
[65] A. Katz, Properties of concrete made with recycled aggregate from partially hydrated old concrete, Cement and Concrete Research. 33 (2003) 703–711. https://doi.org/10.1016/S0008-8846(02)01033-5.
[66] H. Loria, P. Pereira-Almao, M. Satyro, Prediction of Density and Viscosity of Bitumen Using the Peng−Robinson Equation of State, Industrial & Engineering Chemistry Research. 48 (2009) 10129–10135. https://doi.org/10.1021/ie901031n.
[67] European Committee for Standardization, Tests for mechanical and physical properties of aggregates - Part 4: Determination of the voids of dry compacted filler, 2008.
[68] European Committee for Standardization, Methods of testing cement - Part 1: Determination of strength, 2016.
[69] European Committee for Standardization, Characterisation of waste - Leaching - Compliance test for leaching of granular waste materials and sludges - Part 2: One stage batch test at a liquid to solid ratio of 10 l/kg for materials with particle size below 4 mm (without or with size reduction), 2004.
[70] European Committee for Standardization, Water quality - Determination of dissolved anions by liquid chromatography of ions - Part 1: Determination of bromide, chloride, fluoride, nitrate, nitrite, phosphate and sulfate, 2009.
[71] European Committee for Standardization, Water quality - Application of inductively coupled plasma mass spectrometry (ICP-MS) - Part 2: Determination of selected elements including uranium isotopes, 2016.
[72] European Parliament, Council Decision of 19 December 2002 establishing criteria and procedures for the acceptance of waste at landfills pursuant to Article 16 of and Annex II to Directive 1999/31/EC, 2003.

[73] V. Letelier, J. Ortega, P. Muñoz, E. Tarela, G. Moriconi, Influence of Waste Brick Powder in the Mechanical Properties of Recycled Aggregate Concrete, Sustainability. 10 (2018) 1037. https://doi.org/10.3390/su10041037.
[74] M. Choquette, M.-A. Berube, J. Locat, Behavior of common rock-forming minerals in a strongly basic NaOH solution, The Canadian Mineralogist. 29 (1991) 163–173.
[75] I.G. Richardson, G.W. Groves, The structure of the calcium silicate hydrate phases present in hardened pastes of white Portland cement/blast-furnace slag blends, Journal of Materials Science. 32 (1997) 4793–4802. https://doi.org/10.1023/A:1018639232570.
[76] S. Ahmari, X. Ren, V. Toufigh, L. Zhang, Production of geopolymeric binder from blended waste concrete powder and fly ash, Construction and Building Materials. 35 (2012) 718–729. https://doi.org/10.1016/j.conbuildmat.2012.04.044.
[77] C.K. Yip, G.C. Lukey, J.S.J. van Deventer, The coexistence of geopolymeric gel and calcium silicate hydrate at the early stage of alkaline activation, Cement and Concrete Research. 35 (2005) 1688–1697. https://doi.org/10.1016/j.cemconres.2004.10.042.
[78] K. Dombrowski, A. Buchwald, M. Weil, The influence of calcium content on the structure and thermal performance of fly ash based geopolymers, J Mater Sci. 42 (2007) 3033–3043. https://doi.org/10.1007/s10853-006-0532-7.
[79] J. Temuujin, A. van Riessen, R. Williams, Influence of calcium compounds on the mechanical properties of fly ash geopolymer pastes, Journal of Hazardous Materials. 167 (2009) 82–88. https://doi.org/10.1016/j.jhazmat.2008.12.121.
[80] K.J.D. MacKenzie, M.E. Smith, A. Wong, A multinuclear MAS NMR study of calcium-containing aluminosilicate inorganic polymers, J. Mater. Chem. 17 (2007) 5090–5096. https://doi.org/10.1039/B712922J.
[81] M. Falah, R. Obenaus-Emler, P. Kinnunen, M. Illikainen, Effects of Activator Properties and Curing Conditions on Alkali-Activation of Low-Alumina Mine Tailings, Waste Biomass Valor. 11 (2020) 5027–5039. https://doi.org/10.1007/s12649-019-00781-z.
[82] B. Coppola, P. Palmero, L. Montanaro, J.-M. Tulliani, Alkali-activation of marble sludge: Influence of curing conditions and waste glass addition, Journal of the European Ceramic Society. 40 (2020) 3776–3787. https://doi.org/10.1016/j.jeurceramsoc.2019.11.068.
[83] D.E. Ortega-Zavala, J.L. Santana-Carrillo, O. Burciaga-Díaz, J.I. Escalante-García, An initial study on alkali activated limestone binders, Cement and Concrete Research. 120 (2019) 267–278. https://doi.org/10.1016/j.cemconres.2019.04.002.
[84] C.K. Yip, J.S.J. van Deventer, Microanalysis of calcium silicate hydrate gel formed within a geopolymeric binder, Journal of Materials Science. 38 (2003) 3851–3860. https://doi.org/10.1023/A:1025904905176.
[85] A. Bentur, R.L. Berger, J.H. Kung, N.B. Milestone, J.F. Young, Structural Properties of Calcium Silicate Pastes: II, Effect of Curing Temperature, Journal of the American Ceramic Society. 62 (1979) 362–366. https://doi.org/10.1111/j.1151-2916.1979.tb19079.x.
[86] D.P. Bentz, P.E. Stutzman, F. Zunino, Low-temperature curing strength enhancement in cement-based materials containing limestone powder, Mater Struct. 50 (2017) 173. https://doi.org/10.1617/s11527-017-1042-6.
[87] I. Elkhadiri, M. Palacios, F. Puertas, Effect of curing temperatura on hydration process of different cement, Ceramics - Silikáty. 53 (2009) 65–75.
[88] A. Fernandez-Jimenez, F. Puertas, Effect of activator mix on the hydration and strength behaviour of alkali-activated slag cements, Advances in Cement Research. (2003) 8.
[89] E. Kamseu, M.C. Bignozzi, U.C. Melo, C. Leonelli, V.M. Sglavo, Design of inorganic polymer cements: Effects of matrix strengthening on microstructure, Construction and Building Materials. 38 (2013) 1135–1145. https://doi.org/10.1016/j.conbuildmat.2012.09.033.
[90] M.L. Granizo, M.T. Blanco-Varela, S. Martínez-Ramírez, Alkali activation of metakaolins: parameters affecting mechanical, structural and microstructural properties, Journal of Materials Science. 42 (2007) 2934–2943. https://doi.org/10.1007/s10853-006-0565-y.
[91] N. Yamaguchi, K. Ikeda, Preparation of geopolymeric materials from sewage sludge slag with special emphasis to the matrix compositions, Journal of the Ceramic Society of Japan. 118 (2010) 107–112. https://doi.org/10.2109/jcersj2.118.107.

[92] C. Lampris, R. Lupo, C.R. Cheeseman, Geopolymerisation of silt generated from construction and demolition waste washing plants, Waste Management. 29 (2009) 368–373. https://doi.org/10.1016/j.wasman.2008.04.007.
[93] V.K. Jha, A. Tuladhar, An attempt of geopolymer synthesis from construction waste, Journal of Nepal Chemical Society. 28 (2013) 29–33.
[94] H. Xu, J.S.J. Van Deventer, Geopolymerisation of multiple minerals, Minerals Engineering. 15 (2002) 1131–1139. https://doi.org/10.1016/S0892-6875(02)00255-8.
[95] X. Zhou, D. Liu, H. Bu, L. Deng, H. Liu, P. Yuan, P. Du, H. Song, XRD-based quantitative analysis of clay minerals using reference intensity ratios, mineral intensity factors, Rietveld, and full pattern summation methods: A critical review, Solid Earth Sciences. 3 (2018) 16–29. https://doi.org/10.1016/j.sesci.2017.12.002.
[96] D. Khale, R. Chaudhary, Mechanism of geopolymerization and factors influencing its development: a review, Journal of Materials Science. 42 (2007) 729–746. https://doi.org/10.1007/s10853-006-0401-4.
[97] P. Giannaros, A. Kanellopoulos, A. Al-Tabbaa, Sealing of cracks in cement using microencapsulated sodium silicate, Smart Mater. Struct. 25 (2016) 084005. https://doi.org/10.1088/0964-1726/25/8/084005.
[98] C.-S. Poon, X.C. Qiao, D. Chan, The cause and influence of self-cementing properties of fine recycled concrete aggregates on the properties of unbound sub-base, Waste Management. 26 (2006) 1166–1172. https://doi.org/10.1016/j.wasman.2005.12.013.
[99] P.-C. Aïtcin, R.J. Flatt, Science and technology of concrete admixtures, Woodhead Publishing, Cambridge, UK, 2016.
[100] M. Arm, Self-cementing properties of crushed demolished concrete in unbound layers: results from triaxial tests and field tests, Waste Management. 21 (2001) 235–239. https://doi.org/10.1016/S0956-053X(00)00095-7.
[101] F. Puertas, M. Palacios, H. Manzano, J.S. Dolado, A. Rico, J. Rodríguez, A model for the C-A-S-H gel formed in alkali-activated slag cements, Journal of the European Ceramic Society. 31 (2011) 2043–2056. https://doi.org/10.1016/j.jeurceramsoc.2011.04.036.
[102] R. Embong, A. Kusbiantoro, N. Shafiq, M.F. Nuruddin, Strength and microstructural properties of fly ash based geopolymer concrete containing high-calcium and water-absorptive aggregate, Journal of Cleaner Production. 112 (2016) 816–822. https://doi.org/10.1016/j.jclepro.2015.06.058.
[103] N. Cristelo, A. Fernández-Jiménez, C. Vieira, T. Miranda, Á. Palomo, Stabilisation of construction and demolition waste with a high fines content using alkali activated fly ash, Construction and Building Materials. 170 (2018) 26–39. https://doi.org/10.1016/j.conbuildmat.2018.03.057.
[104] Q. Pu, L. Jiang, J. Xu, H. Chu, Y. Xu, Y. Zhang, Evolution of pH and chemical composition of pore solution in carbonated concrete, Construction and Building Materials. 28 (2012) 519–524. https://doi.org/10.1016/j.conbuildmat.2011.09.006.
[105] T.-W. Feng, J.-Y. Lee, Y.-J. Lee, Consolidation behavior of a soft mud treated with small cement content, Engineering Geology. 59 (2001) 327–335. https://doi.org/10.1016/S0013-7952(01)00021-7.
[106] F. Ungaro, F. Ragazzi, R. Cappellin, P. Giandon, Arsenic concentration in the soils of the Brenta Plain (Northern Italy): Mapping the probability of exceeding contamination thresholds, Journal of Geochemical Exploration. (2008) 15.
[107] M. Bassani, F. Bertola, M. Bianchi, F. Canonico, M. Marian, Environmental assessment and geomechanical properties of controlled low-strength materials with recycled and alternative components for cements and aggregates, Cement and Concrete Composites. 80 (2017) 143–156. https://doi.org/10.1016/j.cemconcomp.2017.03.013.
[108] I. Del Rey, J. Ayuso, A.P. Galvín, J.R. Jiménez, M. López, M.L. García-Garrido, Analysis of chromium and sulphate origins in construction recycled materials based on leaching test results, Waste Management. 46 (2015) 278–286. https://doi.org/10.1016/j.wasman.2015.07.051.
[109] A.P. Galvín, J. Ayuso, I. García, J.R. Jiménez, F. Gutiérrez, The effect of compaction on the leaching and pollutant emission time of recycled aggregates from construction and demolition waste, Journal of Cleaner Production. 83 (2014) 294–304. https://doi.org/10.1016/j.jclepro.2014.07.074.
[110] I.M. Milagre-Martins, A.J. Roque, A.C. Freire, J. Neves, M.L. Antunes, Release of dangerous substances from construction and demolition recycled materials used in road pavements-Laboratory and field leaching tests, in: III Progress of Recycling in the Built Environment, RILEM Publications SARL, 2015: pp. 109–115.

[111] Y.-C. Jang, T. Townsend, Sulfate leaching from recovered construction and demolition debris fines, Advances in Environmental Research. 5 (2001) 203–217. https://doi.org/10.1016/S1093-0191(00)00056-3.
[112] A.J. Roque, I.M. Martins, A.C. Freire, J.M. Neves, M.L. Antunes, Assessment of Environmental Hazardous of Construction and Demolition Recycled Materials (C&DRM) from Laboratory and Field Leaching Tests Application in Road Pavement Layers, Procedia Engineering. 143 (2016) 204–211. https://doi.org/10.1016/j.proeng.2016.06.026.
[113] A. Barbudo, F. Agrela, J. Ayuso, J.R. Jiménez, C.S. Poon, Statistical analysis of recycled aggregates derived from different sources for sub-base applications, Construction and Building Materials. 28 (2012) 129–138. https://doi.org/10.1016/j.conbuildmat.2011.07.035.
[114] W.E. Brownell, Application of New Techniques to the Solution of an Efflorescence Problem, Journal of the American Ceramic Society. (1950). https://doi.org/10.1111/j.1151-2916.1950.tb14152.x.
[115] A. Andrés, M.C. Díaz, A. Coz, M.J. Abellán, J.R. Viguri, Physico-chemical characterisation of bricks all through the manufacture process in relation to efflorescence salts, Journal of the European Ceramic Society. 29 (2009) 1869–1877. https://doi.org/10.1016/j.jeurceramsoc.2008.11.015.
[116] N. Saca, Al. Dimache, L.R. Radu, I. Iancu, Leaching behavior of some demolition wastes, Journal of Material Cycles and Waste Management. 19 (2017) 623–630. https://doi.org/10.1007/s10163-015-0459-7.
[117] K.C. Vrancken, B. Laethem, Recycling options for gypsum from construction and demolition waste, in: Waste Management Series, Elsevier, 2000: pp. 325–331. https://doi.org/10.1016/S0713-2743(00)80045-8.
[118] P. Kijjanapanich, A.T. Do, A.P. Annachhatre, G. Esposito, D.H. Yeh, P.N.L. Lens, Biological sulfate removal from construction and demolition debris leachate: Effect of bioreactor configuration, Journal of Hazardous Materials. 269 (2014) 38–44. https://doi.org/10.1016/j.jhazmat.2013.10.015.
[119] P. Kijjanapanich, A.P. Annachhatre, G. Esposito, P.N.L. Lens, Chemical sulphate removal for treatment of construction and demolition debris leachate, Environmental Technology. 35 (2014) 1989–1996. https://doi.org/10.1080/09593330.2014.889219.
[120] P. Duxson, S.W. Mallicoat, G.C. Lukey, W.M. Kriven, J.S.J. van Deventer, The effect of alkali and Si/Al ratio on the development of mechanical properties of metakaolin-based geopolymers, Colloids and Surfaces A: Physicochemical and Engineering Aspects. 292 (2007) 8–20. https://doi.org/10.1016/j.colsurfa.2006.05.044.
[121] H.A. van der Sloot, J.C.L. Meeussen, A. van Zomeren, D.S. Kosson, Developments in the characterisation of waste materials for environmental impact assessment purposes, Journal of Geochemical Exploration. 88 (2006) 72–76. https://doi.org/10.1016/j.gexplo.2005.08.092.
[122] A.P. Galvín, J. Ayuso, J.R. Jiménez, F. Agrela, Comparison of batch leaching tests and influence of pH on the release of metals from construction and demolition wastes, Waste Management. 32 (2012) 88–95. https://doi.org/10.1016/j.wasman.2011.09.010.
[123] M.B. Maia, J. De Brito, I.M. Martins, J.D. Silvestre, Toxicity of Recycled Concrete Aggregates: Review on Leaching Tests, The Open Construction and Building Technology Journal. 12 (2018) 187–196. https://doi.org/10.2174/1874836801812010187.
[124] K. Komonweeraket, B. Cetin, A.H. Aydilek, C.H. Benson, T.B. Edil, Effects of pH on the leaching mechanisms of elements from fly ash mixed soils, Fuel. 140 (2015) 788–802. https://doi.org/10.1016/j.fuel.2014.09.068.
[125] J.G.S. Van Jaarsveld, J.S.J. Van Deventer, L. Lorenzen, The potential use of geopolymeric materials to immobilise toxic metals: Part I. Theory and applications, Minerals Engineering. 10 (1997) 659–669. https://doi.org/10.1016/S0892-6875(97)00046-0.
[126] Z. Zhang, H. Wang, J.L. Provis, Quantitative study of the reactivity of fly ash in geopolymerization by FTIR, Journal of Sustainable Cement-Based Materials. 1 (2012) 154–166. https://doi.org/10.1080/21650373.2012.752620.
[127] S. Butera, S. Trapp, T.F. Astrup, T.H. Christensen, Soil retention of hexavalent chromium released from construction and demolition waste in a road-base-application scenario, Journal of Hazardous Materials. 298 (2015) 361–367. https://doi.org/10.1016/j.jhazmat.2015.06.025.
[128] J.R. Jiménez, J. Ayuso, F. Agrela, M. López, A.P. Galvín, Utilisation of unbound recycled aggregates from selected CDW in unpaved rural roads, Resources, Conservation and Recycling. 58 (2012) 88–97. https://doi.org/10.1016/j.resconrec.2011.10.012.

[129] T.G. Townsend, Y.-C. Jang, T. Tolaymat, Leaching Tests for Evaluating Risk in Solid Waste Management Decision Making, The Florida Center for Solid and Hazardous Waste Management, Gainesville, Florida, US, 2003.
[130] R.W. Peters, Chelant extraction of heavy metals from contaminated soils, Journal of Hazardous Materials. 66 (1999) 151–210. https://doi.org/10.1016/S0304-3894(99)00010-2.
[131] H.A. Van der Sloot, Developments in evaluating environmental impact from utilization of bulk inert wastes using laboratory leaching tests and field verification, Waste Management. 16 (1996) 65–81. https://doi.org/10.1016/S0956-053X(96)00028-1.